HETEROCYCLES, Vol. 76, No. 1, 2008, pp. 353 - 380. © The Japan Institute of Heterocyclic Chemistry
Received, 21st January, 2008, Accepted, 17th March, 2008, Published online, 18th March, 2008. COM-08-S(N)14

THE OCTAETHYLPORPHYRIN-DIHEXYLBITHIOPHENE DERIVATIVES COMBINED WITH PYRIDINE AND PYRIMIDINE RINGS. THEIR SYNTHESES AND PROTON-MEDIATED AND HEAT-DRIVEN SPECTRAL CHANGES

Hiroyuki Higuchi,[a]* Naoto Hayashi,[a] Takuya Matsukihira,[a] Takanori Kawakami,[b] Toru Takizawa,[c] Junji Saito,[d] Keiko Miyabayashi,[e] and Mikio Miyake[e]

[a]Graduate School of Science and Engineering, University of Toyama, 3190 Gofuku, Toyama, Toyama 930-8555, Japan
[b]Water Quality Management Center, University of Toyama, 3190 Gofuku, Toyama, Toyama 930-8555, Japan
[c]Nicca Chemical Co., Ltd., 23-1-4 Bunkyo, Fukui, Fukui 910-8670, Japan
[d]Tateyama Kagaku Ind. Co., Ltd., 30 Shimonoban, Oyama, Kami-niikawa, Toyama, Toyama 930-1305, Japan
[e]School of Material Science, JAIST (Hokuriku), 1-1 Asahi-dai, Tatsunokuchi, Noumi, Ishikawa 923-1292, Japan

Abstract - The octaethylporphyrin (OEP)-dihexylbithiophene (DHBTh) derivatives combined with pyridine (Pyr) and pyrimidine (Pym) as proton-acceptable rings (PAR) were synthesized, describable as OEP-DHBTh-PAR, in which all the OEP, DHBTh, and PAR components are connected with diacetylene linkage. Their ^{1}H NMR and electronic spectral properties and electrochemical behaviors were studied under the neutral and acidic conditions. Reversible proton-mediated and heat-driven spectral changes of OEP- DHBTh-PAR were performed, reflecting both properties of PAR and DHBTh.

INTRODUCTION

In order to develop the new organic functional materials for supporting the present photo-electronics society life, a variety of heterocycle-nucleic conjugation systems have been vastly demonstrated, by virtue of their high susceptibilities to the outside stimulations such as optical and electronic effects.[1] Among them, a group of porphyrin derivatives which reversibly exchange their structures and/or spectral properties responding to those outside stimulations is highly promising for the functional materials such as photo-switches[2] and molecular-recognition reagents.[3] In connection with such a drastic development of the functional material researches of porphyrin-based π-electronic systems, we previously synthesized the diacetylene-group connected octaethylporphyrin-dihexylbithiophene-(4)pyridine derivatives **1** and **2**

(Chart 1), in which the dihexylbithiophene (DHBTh) ring possesses head-to-head (HH) or tail-to-tail (TT) orientation.[4] In that study, the electronic properties of octaethylporphyrin (OEP) nucleus at one terminal site of the molecule were figured out under such acidic conditions as to protonate fully onto pyridine (Pyr) ring at another terminal site. Especially from the experiments of electronic spectral properties, it was proved that these OEP(Ni) derivatives showed the dramatic change between neutral and acidic conditions with reflecting their orientations of DHBTh, and was suggested that their spectra changed via two steady-state processes. Yet, an outstanding peak-broadening phenomenon in their ^{1}H NMR spectra was observed only for the particular protons under sufficiently acidic conditions. The reason for this peculiarity in peak-broadness is still uncertain.

These preliminary investigations of **1** and **2** strongly stimulated us to continue further quantitative analysis of the protonation effect on ^{1}H NMR and electronic spectral properties of the OEP-DHBTh-(4)Pyr system. Also, in order to ascertain a generality for the above spectral properties, the OEP-DHBTh derivatives **3** and **4** have been synthesized, in which the Pyr ring is combined at its 2-position, describable as OEP-DHBTh-(2)Pyr (Chart 1). On the way of construction of **4**, an unexpected compound was produced as a main product under the same reaction conditions as for **2**, though the desired compound **4** could be obtained after several trials. Subsequently, in order to evaluate an effect of the proton-acceptable ring (PAR) on the spectral properties, the OEP-DHBTh derivatives **5** and **6** have been synthesized, in which the much less basic pyrimidine (Pym) ring is combined at 2-position, describable as OEP-DHBTh-(2)Pym. Furthermore, in order to clarify the respective species to each steady-state spectrum upon addition of acid into **1** and **2**, the corresponding (4)Pyr(N-methylated) derivatives **7** and **8** have been synthesized, which are simply described as OEP-DHBTh-(4)Pyr(NMe)I (Chart 1).

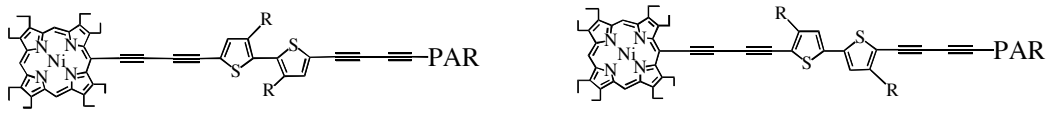

OEP-(HH)DHBTh-PAR $R=C_6H_{13}$ OEP-(TT)DHBTh-PAR

PAR		PAR	
1:		**2:**	
3:		**4:**	
5:		**6:**	
7:	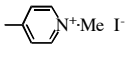	**8:**	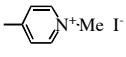

Chart 1

In this paper, the syntheses of the OEP-DHBTh-PAR derivatives **1**-**8** connected with diacetylene linkage and their structural and spectral aspects will be described, together with the orientation effect of DHBTh on their electronic properties. Then, it is briefly discussed that the present system potentially behaves as a molecular machine,[1,2,3] reversibly exchangeable between more than two structures by means of proton- and heat-stimulations.

RESULTS AND DISCUSSION

1. SYNTHESES OF OEP-DHBTh-PAR DERIVATIVES 1-8. According to Eglinton method,[5] synthesis of the diacetylene-group connected compounds **1**-**6** was planned by oxidative cross-coupling of the terminal acetylenes of **9**[6] and **10**[6] with **11**,[7] **12**[7] or **13**, as shown in Scheme 1. The (4)Pyr terminal acetylene **11** is hard to exist in a free form for a long reaction period under such an oxidative atmosphere, spontaneously affording the diacetylene-group connected (4)Pyr dimer **14**[8] (Chart 2). Therefore, the hydrochloride of **11** was employed for the coupling reaction as it was, with more than 10 times excessively equivalent (eq.) molar amount to **9** or **10**. In practice, our modified binary solvent system [Pyr : methanol (MeOH)=1:1][9] was found useful for gradual generation of the free acetylene **11**. The coupling reaction of **11** with the corresponding OEP-DHBTh acetylenes **9** and **10** smoothly took place in the presence of copper(II) diacetate [$Cu(OAc)_2$] to afford the derivatives **1** and **2** in moderate yields, respectively, together with a considerable amount of **14** and a small amount of homo-coupling dimer **15** or **16** (Chart 2).[10]

On the other hand, fortunately, the (2)Pyr terminal acetylene **12** is stable enough to be handled in an ordinary aerial atmosphere, as it is. However, the consequence for **3** and **4** was entirely different from that for **1** and **2**. For example, the coupling reaction of **12** with **10** under the same conditions as for **2** did not produce the desired product **4** at all, but afforded the derivative **17** substituted with OMe group in place of the (2)Pyr ring (Chart 2). This result indicates that the solvent molecule of MeOH participated in this reaction somehow (vide infra). Therefore, when the coupling reaction between **10** and **12** was carried out in a sole solvent of Pyr,[5] the desired product **4** could be obtained in a good yield, as well as the HH isomer **3** from **9** and **12**. Similarly, coupling reactions of the (2)Pym terminal acetylene **13** with **9** and **10** in Pyr solvent afforded **5** and **6** in adequate yields, respectively.

Then, the reaction of **1** and **2** with methyl iodide (MeI) in acetone was carried out with gentle reflux in a sealed tube, to afford the OEP-DHBTh-(4)Pyr(NMe)I derivatives **7** and **8** in quantitative yields, respectively. All the OEP-DHBTh-PAR derivatives **1**-**8** thus obtained are black purple microcrystals and are stable enough to be stored at room temperature for more than 2 year.

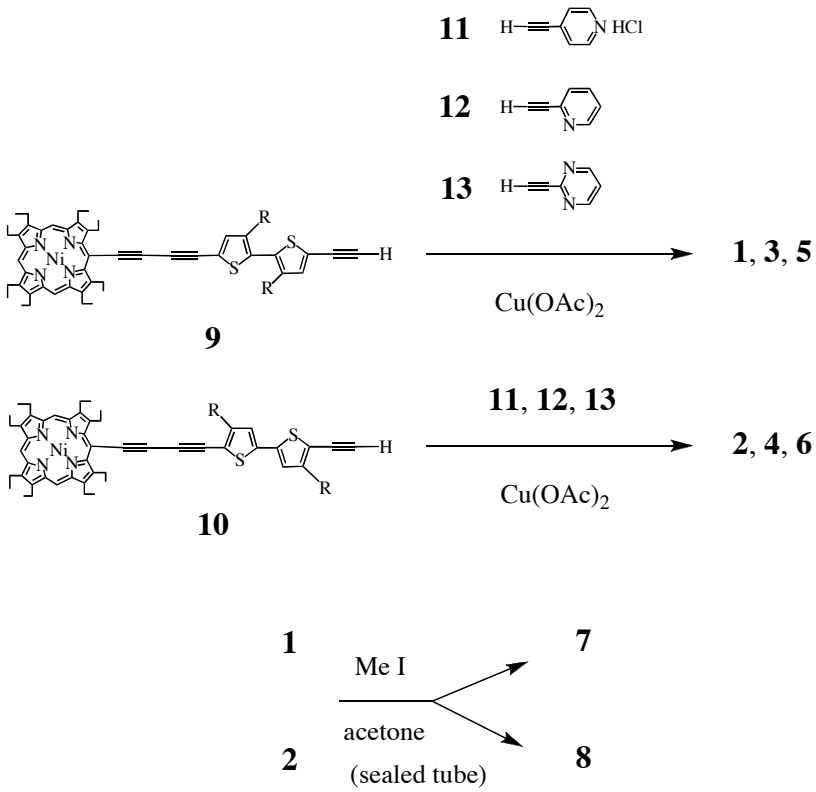

Scheme 1

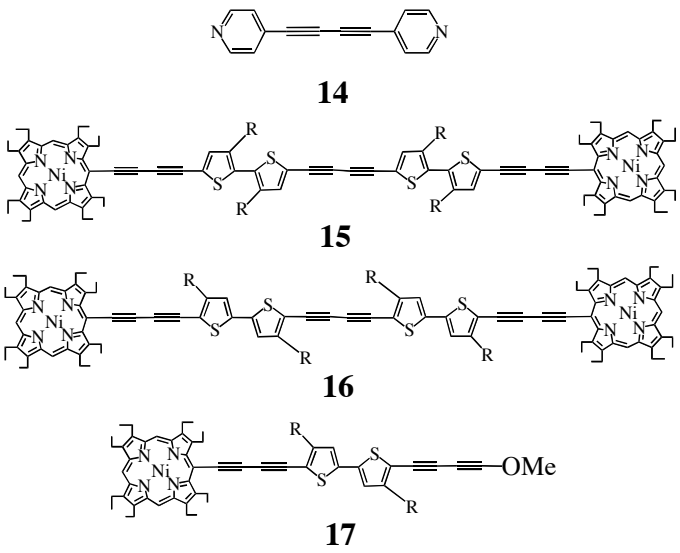

Chart 2

2. STRUCTURE DETERMINATIONS AND CHARACTERIZATIONS OF 1-8. All the structures of OEP-DHBTh-PAR derivatives as well as related compounds were definitely determined by means of MS, IR, and ^{1}H NMR spectral measurements, together with their satisfactory elemental analyses. In IR spectra, similarly to the case of other OEP-DHBTh systems,[6,11] the stretching vibrations due to the diacetylene group appeared at the lower wave-numbers in the (TT)DHBTh isomers than those in the corresponding (HH)DHBTh isomers. For example, the (HH)DHBTh derivative **1** showed a set of two typical absorptions at 2200 (m) and 2130 cm^{-1} (w), while the (TT)DHBTh derivative **2** showed them at 2196 and 2122 cm^{-1}. The corresponding (4)Pyr(NMe)I derivatives also exhibited the same trend with both further lower energy shifts, to afford 2191 and 2128 cm^{-1} for HH isomer **7** and 2180 and 2123 cm^{-1} for TT isomer **8**. These results clearly show that the diacetylene linkage takes part in the π-electronic conjugation throughout the molecules in a (TT)DHBTh series more efficiently, because of their higher molecular planarity (vide infra).[6b, 12]

In ^{1}H NMR spectra, all derivatives **1**-**8** exhibited fairly simple features, affording two singlet meso-proton (meso-H) peaks of OEP, two singlet thiophene-proton (Th-H) peaks of DHBTh, and respective proton peaks of the terminal PAR, respectively. Other ethyl and hexyl substituents on the skeletal periphery also afforded their corresponding proton peaks with the same splitting patterns as those in each component. The spectra of **2** as well as its related compounds **10** and **14**, for example, are shown in Figure 1. Meso-H of **2** appeared at around δ=9.4 ppm and its Th-H appeared at around 7.0 ppm, both of which are almost the same as those of the coupling counterpart **10**. With respect to the Pyr ring protons (Pyr-H), the chemical shifts of **2** were also nearly the same as the corresponding ones of **14**. This trend in chemical shifts of respective protons was commonly observed in all other OEP-DHBTh-PAR derivatives.[6] Therefore, between all sets of (HH)- and (TT)DHBTh orientational isomers, only the peaks owing to Th-H can be distinguished from each other, reflecting an anisotropic effect of diacetylene linkage on the respective Th-H with different magnitudes, to appear at the lower field by ca. 0.4 ppm for the (HH)DHBTh derivatives.[4] These results clearly indicate that the diacetylene-group connected system of this type substantially possesses the molecular skeleton of the OEP-DHBTh constituent **9** or **10**, simply being combined with respective PAR, without particularly being affected by an extension of its π-electronic conjugation with PAR. In this respect, it should be noticed that a set of the Pyr(NMe)I isomers **7** and **8** exhibited a considerable difference in their ^{1}H NMR spectra from **1** and **2** (vide infra).

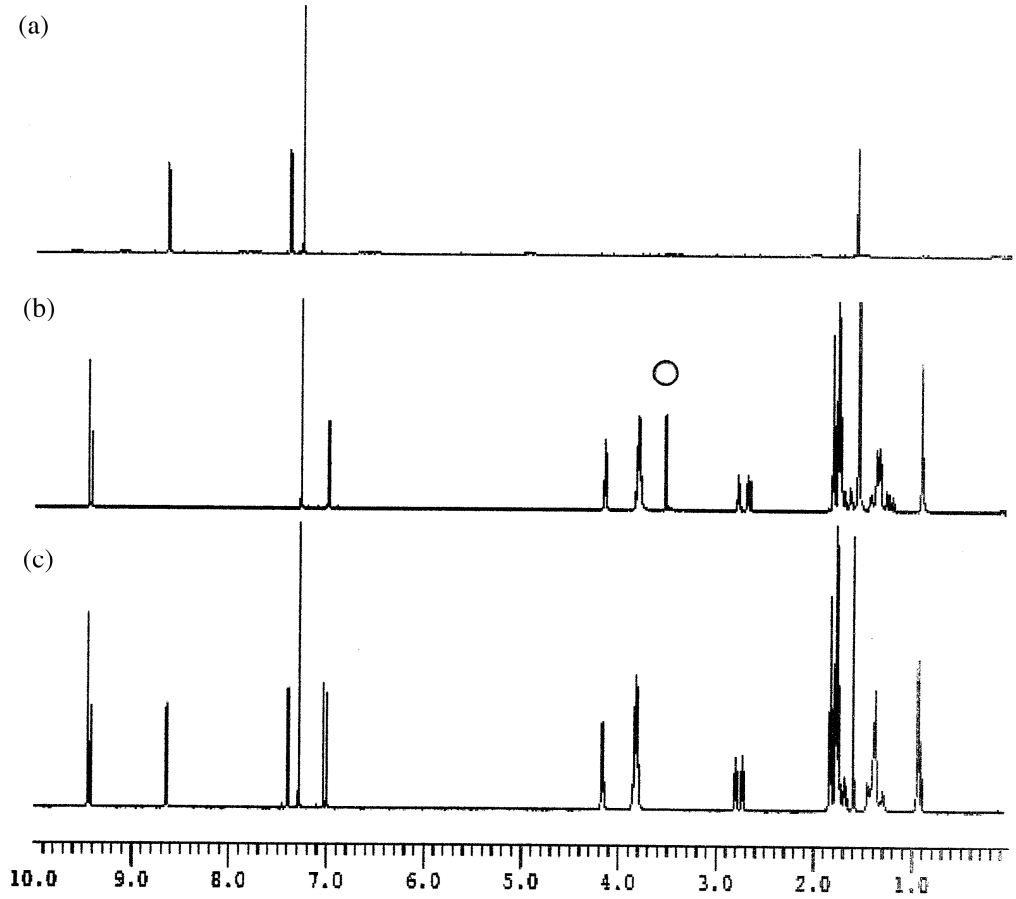

Figure 1. ^{1}H NMR spectra of (a) **14**, (b) **10** and (c) **2** ($CDCl_3$, 600 MHz, at 25 ˚C). Open circle shows the terminal acetylenic proton.

3. SOME PECULIAR FEATURES OF THE OEP-DHBTh-PAR SYSTEM.

3. 1. MeOH ADDUCT FORMATION TO 4. The binary solvent system of Pyr and MeOH (modified Eglinton coupling conditions)[9] is useful for the diacetylene formation in our OEP-DHBTh derivative syntheses. However, in the present solvent system for the OEP-DHBTh-(2)Pyr derivative, the addition reaction of MeOH to **4** took place prior to a simple formation of the dicaetylene linkage. Thus, the coupling of **10** with the (4)Pyr terminal acetylene **11** afforded the normal product **2** in a good yield, while the coupling with the (2)Pyr terminal acetylene **12** under the same conditions did not afford the desired product **4** at all but gave **17** as a major product and **18** as a minor product (Chart 2 and Scheme 2). ^{1}H NMR spectra of **17** and **18** are shown in Figure 2, together with the spectrum of **4** synthesized by an alternative way. It clearly indicates that **17** does not possess the Pyr ring but carries one Me group (δ=3.84 ppm, pointed with filled circle), and that **18** possesses one Me group (δ=4.32 ppm, pointed with filled circle) and one olefinic proton (δ=6.61 ppm, pointed with open circle) in addition to all the protons of **4**. Their IR spectra also showed the stretching vibrations due to conjugated C-C triple bond at ν=2178

and 2128 cm^{-1} for **17** and at ν=2166 and 2126 cm^{-1} for **18**, similar to those (ν=2198 and 2127 cm^{-1}) for **4**. These results clearly show **17** to be the OMe-substituted derivative and **18** to be the MeOH adduct to **4**. Both **17** and **18** were evidently supported by MS spectra as well, affording m/z 1049.4 (**4** – Pyr + MeOH) for **17** and 1128.5 (**4** + MeOH) for **18** as referred to m/z 1095.5 for **4**. Furthermore, by following this reaction with thin-layer chromatography (TLC), it was indicated that the MeOH adduct **18** forms initially and changes into **17** successively.

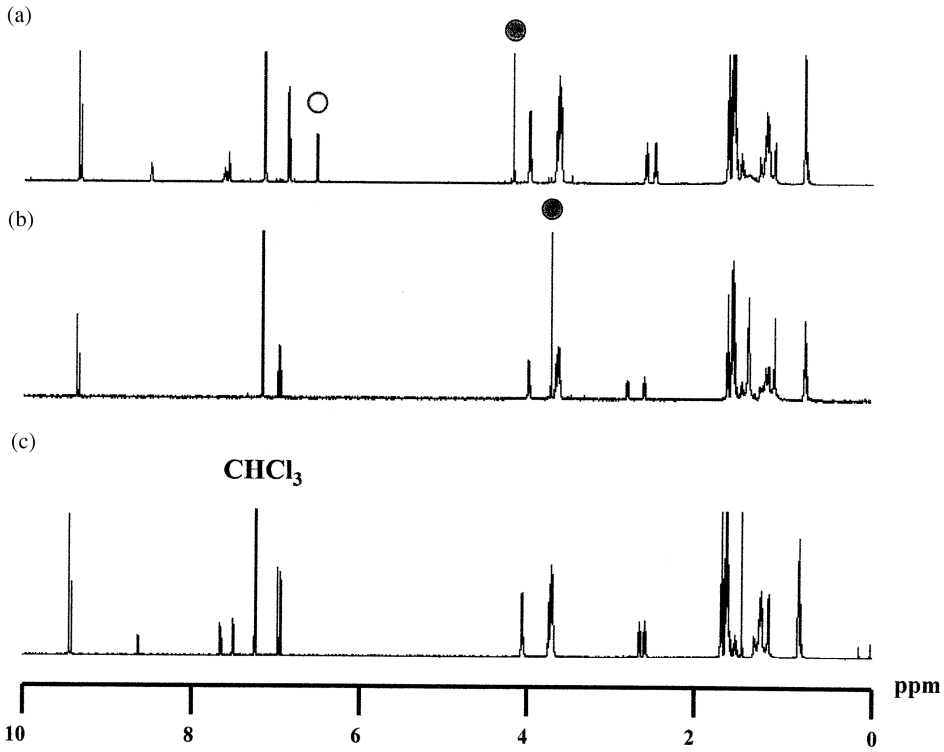

Figure 2. ^{1}H NMR spectra of (a) **18**, (b) **17** and (c) **4** ($CDCl_3$, 600 MHz, at 25 ˚C). Open circle shows the olefinic proton and filled circle shows the OMe protons.

The above curious reaction is expected to proceed by an assistance of the (2)Pyr counterpart itself. In a transition state of the reaction between **10** and **12**, a fully competitive path with the diacetylene linkage formation could be driven by MeOH molecule which is activated with the nearby (2)Pyr-N atom through an unhindered hydrogen bonding, as shown in Scheme 2. As a plausible mechanism, it is proposed that the oxygen atom of MeOH having an enhanced nucleophilicity aligns preferably for attacking the nearest sp-C in the Cu(II)-coordinated acetylene bond, affording **18** prior to **19**. The OMe substituted derivative **17** is likely formed by elimination of the Pyr ring from **18**, where the (2)Pyr-N atom again plays a role for enhancement of acidity of olefinic β-hydrogen. This is not a case for the corresponding (4)Pyr-N atom because of far distance to the Cu(II)-coordinated acetylene bond, resulting in no such nucleophilic attack by MeOH molecule, though an unhindered hydrogen bonding between them would be similarly formed. Yet, in practice, neither **17** nor **18** were produced at all in the absence of MeOH, concluding that this

reaction arises from a stereo-electronically cooperative interaction between acetylene bond, MeOH, and (2)Pyr-N atom. At the present stage, however, it is premature to deduce the reason for *Z*-geometry of MeOH adduct **18** with confidence, which should wait for further investigations.[13]

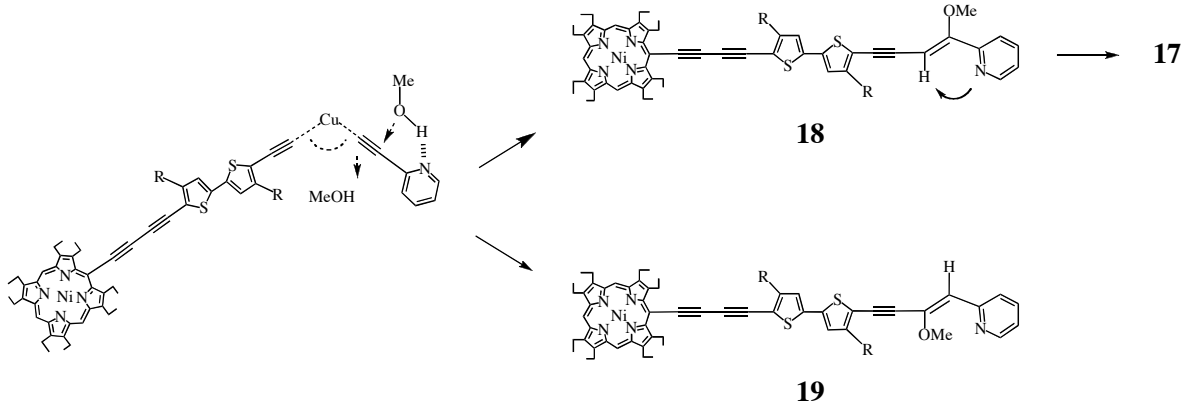

Scheme 2

3. 2. STRUCTURAL CHARACTERISTICS OF 7 AND 8. The OEP-DHBTh-PAR derivatives **1**-**6** proved to be the system substantially possessing the molecular skeleton of the OEP-DHBTh constituent **9** or **10**, simply being combined with respective PAR (vide supra). In case of the (4)Pyr(NMe)I derivatives **7** and **8**, however, their molecular skeletal properties were slightly different from those of the corresponding derivatives **1** and **2**, in consequence of the positive-charge introduction into the Pyr ring. In ^{1}H NMR spectra (Figure 3), the (HH)DHBTh-(4)Pyr(NMe)I derivative **7** substantially exhibited a similar pattern to that of **1**, affording two meso-H (δ=9.44 and 9.42 ppm), two sets of Th-H (δ=7.39 and 7.31 ppm) and two Pyr-H (δ=8.38 and 7.34 ppm) peaks, as shown in Figures 3a and 3b. Both meso-H and Th-H of **7** as well as its ethyl and hexyl protons appeared at almost the same positions as the corresponding ones of **1**, and its Pyr(NMe)-H (δ=3.96 ppm, pointed with filled square) appeared in the midst of ethyl proton peaks of OEP. Here, it may be noted that Pyr-H of **7** shifted to the higher field than those (δ=8.61 and 7.36 ppm) of **1**, though their shifting values are not so large in magnitude. On the other hand, in case of the (TT)DHBTh-(4)Pyr(NMe)I derivative **8**, meso-H appeared at almost the same positions as those of **2**, while both Pyr-H and Pyr(NMe)-H (pointed with filled square) shifted to the much higher field, appearing at δ=7.64 and 6.84 ppm and at δ=3.25 ppm, respectively (Figures 3c and 3d). Similarly, Th-H of **8** were found to shift very slightly to the high field from those of **2**. Yet, the two hexyl methylene-H directly attached on each HTh ring of **8** gathered to fuse into nearly one set of triplet peaks, in contrast with a clear difference between them in **2**.

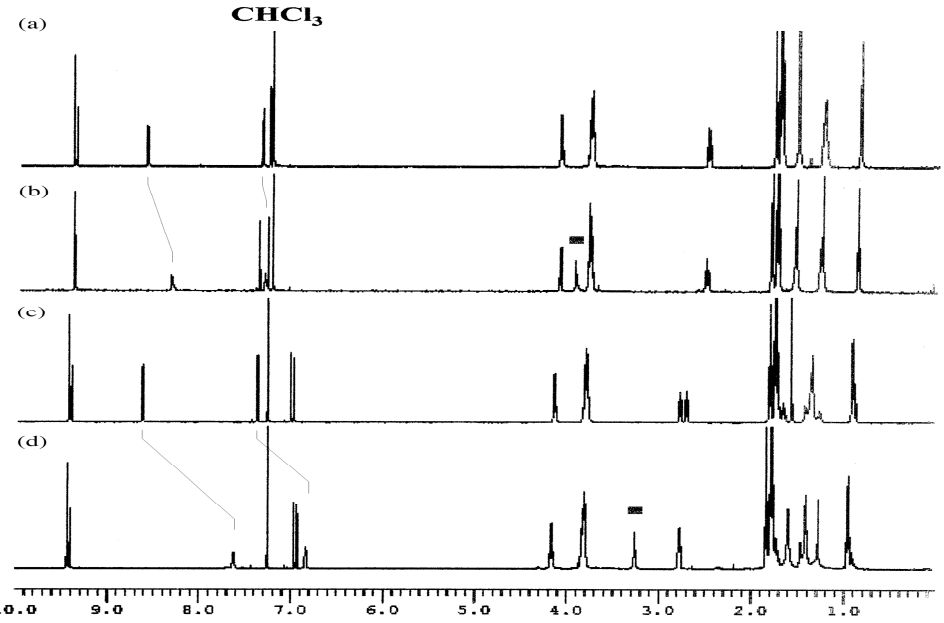

Figure 3. ^{1}H NMR spectra of (a) **1**, (b) **7**, (c) **2** and (d) **8** ($CDCl_3$, 600 MHz, at 25 ˚C). Filled square shows the NMe protons.

In particular, the differences in chemical shifts due to Pyr-H and Pyr(NMe)-H between **7** and **8** are quite large to be more than 0.7 ppm, respectively, in spite of similar circumstances around the (4)Pyr(NMe)I site to each other, suggesting some structural reformation by the positive-charge introduction with reflecting the orientation of DHBTh. Such structural reformation should also bring on the decisive difference in their electronic properties more or less (vide infra). From the above results, at the present stage, it is proposed that the positive-charge delocalization in **7** and **8** could be achieved in some canonical forms such as **20** and **21** as main contributants, as shown in Scheme 3. The greater contribution from **20** and **21** would induce Pyr-H and Pyr(NMe)-H to shift to the higher field, due to the loss of 6 π-electronic cyclic system of the Pyr ring. Based on this thinking, the positive-charge would spread for stabilization through the π-electronic conjugation of **21** over the molecule more efficiently, because of the higher planarity of (TT)DHBTh in **8**.[6b, 12] The cumulative structure of C-C double bonds in **20** and **21** should also lead to the weakness of diacetylene linkage character. In practice, their stretching vibrations shifted to the lower energy regions in order of (**1**>**2**)>(**7**>**8**), as already mentioned in IR spectra. However, it might be excluded to spread the positive-charge onto another terminal OEP ring, since the chemical shifts of meso-H and ethyl protons are nearly the same in all the derivatives **1**, **2**, **7** and **8**.

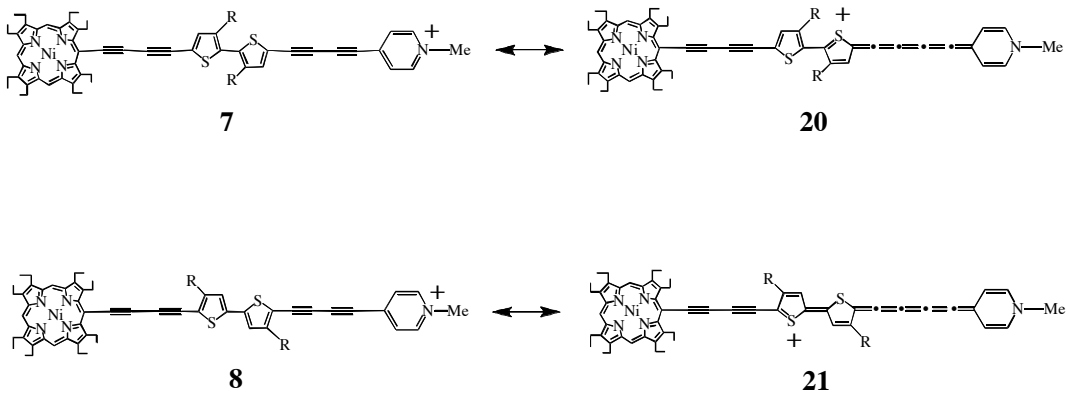

Scheme 3

4. SPECTRAL CHANGES AND ELECTROCHEMICAL BEHAVIORS OF OEP-DHBTh-PAR UNDER NEUTRAL AND ACIDIC CONDITIONS.

4. 1. ^{1}H NMR SPECTRAL EXPERIMENTS. ^{1}H NMR spectral changes of **1**-**6** were successively observed, as follows. Trifluoroacetic acid (TFA, pKa 0.23)[14] was added to a deuterated 1,1,2,2-tetrachloroethane ($CDCl_2CDCl_2$) solution of OEP-DHBTh-PAR, of which the concentrations of each derivative were adjusted equally every measurement. The spectra gradually changed their appearance and finally reached the steady-state, as shown in Figures 4a-d for **2** as a typical example. As seen from the serial spectra, it is revealed that only Pyr-H of **2** gradually change their chemical shifts to the lower field by ca. 0.2 ppm for Ha and ca. 0.5 ppm for Hb, respectively, with other protons including Th-H appearing at almost the same positions as those in 100% $CDCl_2CDCl_2$ solution (Figures 4a and 4b, Scheme 4). In the case of **1**-**4**, at least 1.1-1.3 eq. molar amount of TFA is enough to saturate the chemical shift changes of Pyr-H. As summarized from Table 1, the amount of TFA necessary for saturation of chemical shift changes of PAR-H reflects the basicity of PAR, semi-quantitatively showing the very poor proton-acceptability of **5** and **6**. In addition, it is noted that the peaks due to not only meso-H but also methylene-H of the OEP ethyl substituents enormously broadened or collapsed into the base line by adding more than 1.5 eq. molar amount of TFA, with their chemical shifts themselves unchanged (vide infra). Finally, the original spectrum of **2** was entirely recovered by quenching TFA with triethylamine (NEt_3). These results explicitly indicate that the protonation smoothly occurs at a terminal site of the Pyr ring, simply making the chemical shifts of Pyr-H shift to the lower fields, as depicted in the canonical forms between **A** and **A'** (Scheme 4), and that the π-electronically basic diacetylene linkage is scarcely affected by TFA. Also, other derivatives **1**, **3**, **4**, **5** and **6** substantially exhibited the similar behavior to **2**,

proving that the present derivatives **1**-**6** are regarded as a reversible system to show the proton-mediated spectral changes.

It is interesting to compare the chemical shifts of Pyr-H (Ha; δ=8.62 and Hb; δ=7.37 ppm) of **2** with those between the Pyr(N-protonated) species **2'** and the Pyr(N-methylated) derivative **8**, where both of them formally possess a positive charge on the Pyr constituent. The former **2'** exhibited Pyr-H in a lower field region at δ=8.95 and 8.04 ppm, while the latter **8** exhibited Pyr-H in a higher field region at δ=7.64 and 6.84 ppm (in $CDCl_3$, vide supra). It is apparent that the solvent difference between $CDCl_2CDCl_2$ and $CDCl_3$ scarcely appeared in the chemical shifts of all protons in OEP-DHBTh-PAR. A great difference in chemical shift changes between **2'** and **8** is probably due to the difference in their bond characters, *i.e.*, protonated $^{(+)}$N-H bond and covalent $^{(+)}$N-C bond. In consequence, the character of covalent $^{(+)}$N-C bond is strong enough to pull a trigger of transformation to the canonical structures **20** and **21** (Scheme 3). On the other hand, the character of protonated $^{(+)}$N-H bond is not strong enough to reduce an aromaticity of the Pyr ring in order to achieve an external delocalization of the positive charge.

Table 1. TFA added amount for chemical-shift saturation of PAR-H (600 MHz, $CDCl_2CDCl_2$)[1)]

OEP-DHBTh-PAR	TFA (eq. molar amount to OEP-DHBTh-PAR)
1	1.1
2	1.2
3	1.2
4	1.3
5	41
6	39

1) Each solution of TFA and $CDCl_2CDCl_2$ was adjusted to be totally 0.5 cm^3, which contains ca. 1 mg of OEP-HBTh-PAR (0.9×10^{-3} mmol).

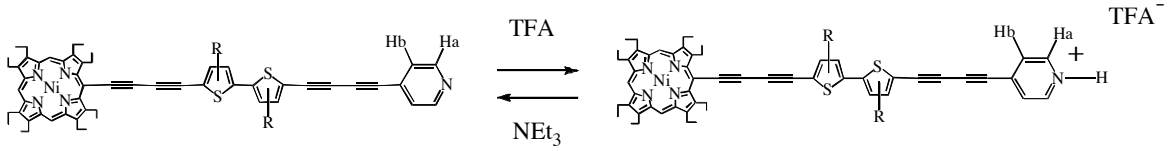

A **A'**

Scheme 4

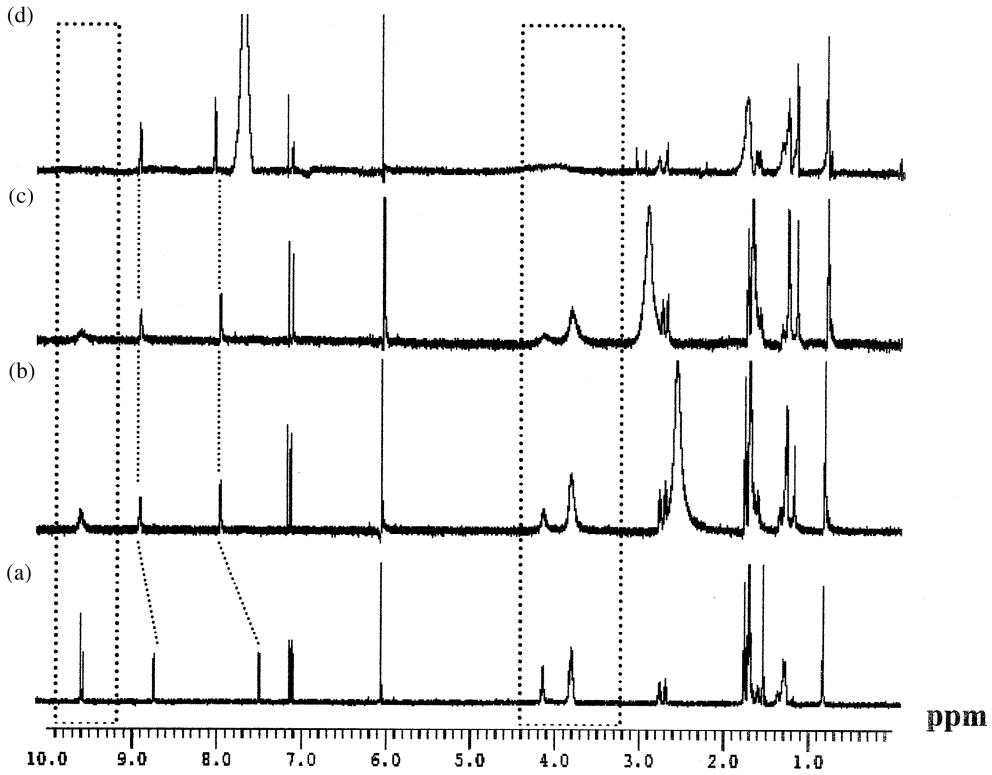

Figure 4. ^{1}H NMR spectral changes of **2** upon addition of TFA into $CDCl_2CDCl_2$ solution (600 MHz, at 25 ˚C). (a) 0.0 eq., (b) 1.5 eq., (c) 2.0 eq., and (d) 2.5 eq. molar amount of TFA to **2**. Each solution (total 0.5 cm^3) contains ca. 1 mg of **2** (see Table 1).

4. 2. ELECTRONIC ABSORPTION SPECTRAL EXPERIMENTS. The electronic absorption spectra of **1**-**6** were initially observed in $CHCl_3$ solutions. The spectra of **1** and **2**, for example, are shown in Figure 5. Reflecting the orientation of DHBTh, HH isomer **1** exhibited one symmetrical curve of Soret band at λ=450 nm, while TT isomer **2** did the broadly distorted Soret band at λ=475 nm together with two shoulder bands in a shorter wavelength region. Compounds **1** and **2** showed the respective Q bands with different shapes from each other, seemingly trapezoidal for **1** and triangular for **2**, but both of them afforded almost the same absorption maximum at around λ=600 nm. These results are highly in accordance with the contrastive roles of the terminal 3-hexylthiophene ring (HTh) of DHBTh in **22** and **23** (Chart 3).[4, 6b, 12] Thus, it could be simply concluded that HH isomer **1** exhibits a combined electronic

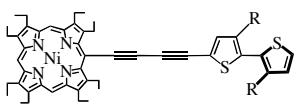

22

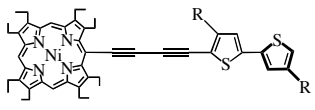

23

Chart 3

structure between two components, *i. e.*, OEP and Pyr chromophores independently interacted with HTh through the diacetylene linkage, describable as [OEP-HTh]-[HTh-Pyr]. On the other hand, TT isomer **2** extends π-electronic conjugation throughout the molecule due to the higher conjugation planarity of (TT)DHBTh.

Addition of TFA to the $CHCl_3$ solutions of **1**-**6** was found to induce the unique changes of their Soret and Q bands more or less. Similar to ^{1}H NMR spectral experiments under the acidic conditions, the concentrations of substrate in solutions were adjusted equally every measurement. A set of serial spectra for **1** and **2**, for example, are shown in Figure 6, both of which proved to change via two stages upon addition of TFA. The first stage is a spectral region changed with less than 10^4~10^5 eq. molar amount of TFA to OEP-DHBTh-PAR and the second stage is a spectral region changed with more than ca. 10^5 eq. molar of TFA. Thus, toward the second steady-state spectra, HH isomer **1** gradually broadened Soret band and decreased its intensity with a small hypsochromic shift from the original band. On the other hand, TT isomer **2** dramatically changed its Soret band to split into two main bands, showing hypsochromic (λ=405 nm) and bathochromic (λ=495 nm) shifts, respectively. In both cases, the initial Q bands in $CHCl_3$ once increased slightly in the first stage, but in the second stage gradually decreased and inversely the new bands increased in a longer wavelength region, appearing at around λ=690 nm for **1** and at around λ=725 nm for **2**, respectively.

The spectral changes of **3** and **4** exhibited almost the same behavior serially as the corresponding ones of **1** and **2** in all respects such as absorption maxima, intensities, and shapes, indicating that the combining position at 2 or 4 of the Pyr component does not affect their electronic structures substantially. In the case of **5** and **6**, their spectra in $CHCl_3$ were also similar to the corresponding spectra of **1** and **2**, exhibiting one symmetrical curve of Soret band at λ=448 nm for **5** and a broadly distorted Soret band at λ=477 nm with a shoulder band for **6** (Figure 7). Yet, the Q bands of **5** and **6** both afforded the absorption maxima at around λ=595 nm, along with the same trend in shape as that of **1** and **2**. Although addition of TFA into the $CHCl_3$ solutions of **5** and **6** induced the similar behavior to other sets of **1**-**4**, their spectral appearance was slightly different from them. In the first stage (less than 10^4~10^5 eq. molar amount of TFA), **5** and **6** exhibited almost the same spectral changes as other sets, while in the second stage (more than 10^7 eq. molar of TFA) both derivatives were found to afford the new Q bands at around λ=700 nm together with very long absorption tails up to 1500 nm. Yet, more than 100 times eq. molar amount of TFA was necessary for **5** and **6** reaching the second steady-state spectra, as compared with **1**-**4**, clearly indicating the poorer proton-acceptability of Pym than Pyr. The molecular structures of **5** and **6** in the second stage should also be the mono-protonated species, in spite of two N atoms in the Pym constituent, since the di-protonated species of the Pym ring is extremely hard to form even in 100% TFA. In accordance with

^{1}H NMR experiments, it was also proved that quenching of TFA with NEt_3 recovered the original spectra of **1**-**6** respectively, without any particular contaminations.

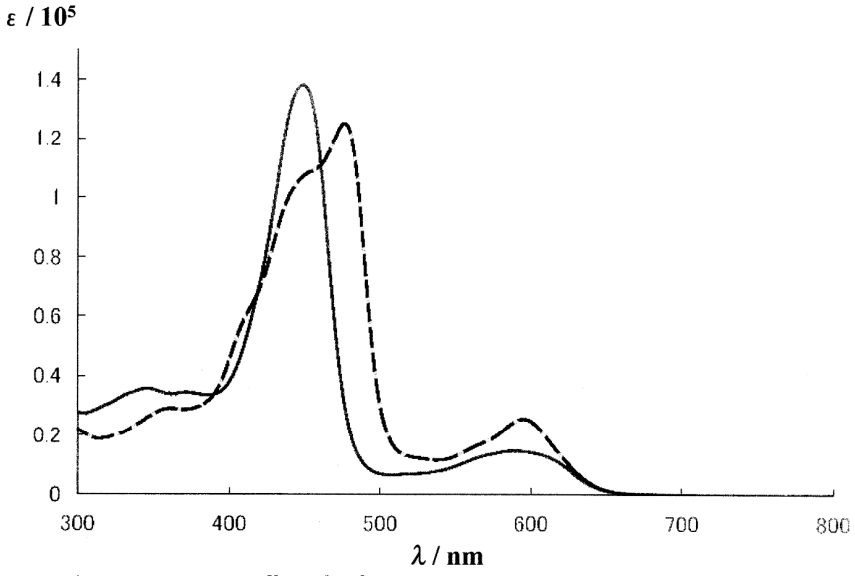

Figure 5. Electronic absorption spectra of **1** (solid line) and **2** (dashed line) ($CHCl_3$, at 25 ˚C).

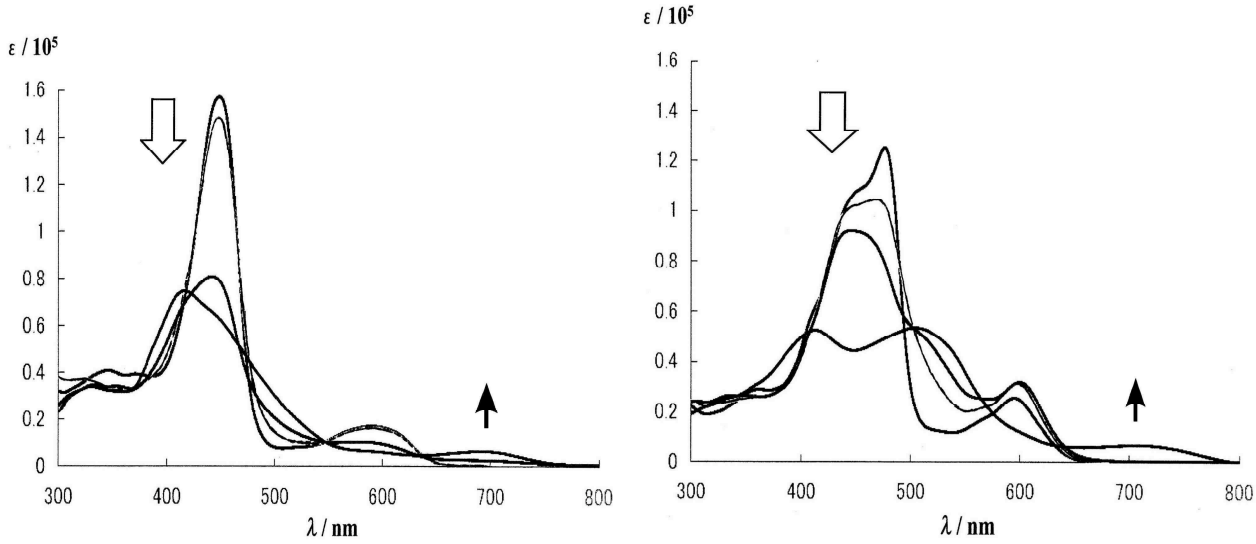

Figure 6. Electronic absorption spectral changes of **1** and **2** upon addition of TFA into $CHCl_3$ solution (25 ˚C). The concentrations of **1** and **2** were adjusted to be 5.0 x 10^{-5} M every measurement. Open arrow shows decreases of Soret band intensity with an increase of TFA content and bold arrow shows increases of the newly appearing Q band intensity. Left side shows spectral changes of **1** with 0 eq., 10^3 eq., 10^5 eq., and 10^6 eq. molar amount of TFA in order. Right side shows spectral changes of **2** with 0 eq., 10^2 eq., 10^3 eq., and 10^4 eq. molar amount of TFA in order.

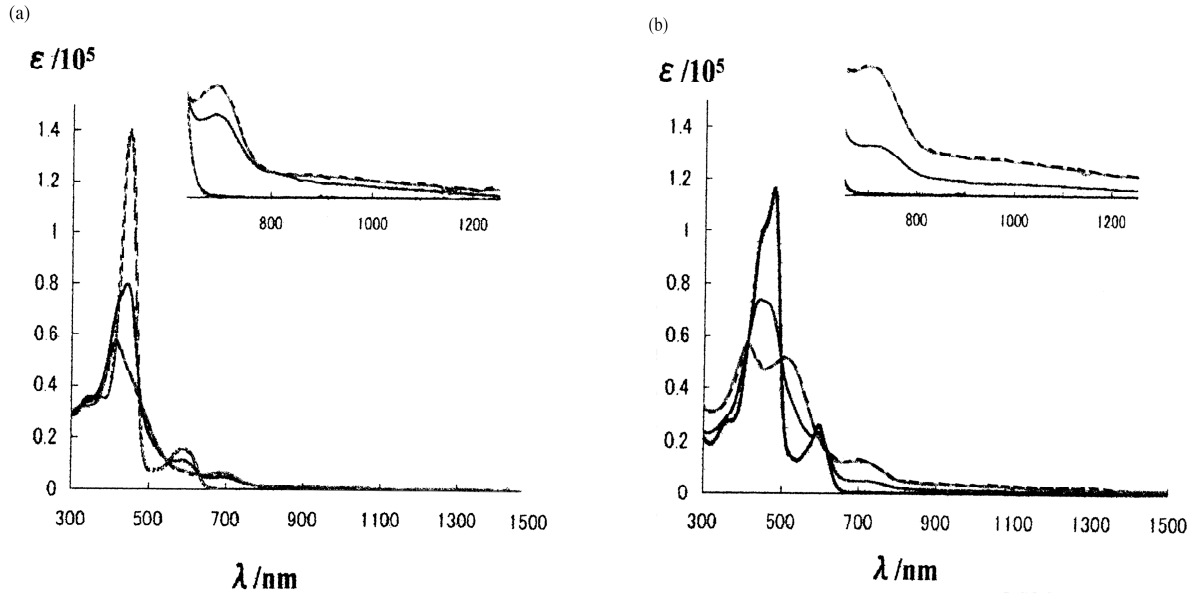

Figure 7. Electronic absorption spectral changes upon addition of TFA into $CHCl_3$ solution (25 ˚C). The concentrations of **5** and **6** were adjusted to be 3.0 x 10^{-5} M every measurement. (a) shows spectral changes of **5** with 0 eq., 10^7 eq., and 10^9 eq. molar amount of TFA in order. (b) shows spectral changes of **6** with 0 eq., 10^7 eq., and 10^9 eq. molar amount of TFA in order. The absorption tails of Q band in the second stage both reached to around 1500 nm.

4. 3. ELECTROCHEMICAL EXPERIMENTS. The studies of electrochemical oxidations of **1**-**8** under various conditions are now in progress,[15] since the electron-releasing ability of the molecule is closely related with various functionalities of the material. The first oxidation potentials as a measure of electron-releasing ability from HOMO level of molecules were measured by cyclic voltammetry (CV) at room temperature. In this paper, the preliminary results of **1** and **2** as well as their Pyr(NMe)I derivatives **7** and **8** are briefly described, especially in connection with their electronic absorption spectra. The first oxidation peak potentials (Ep_1/mV) are summarized in Table 2 and the cyclic voltammograms of **1** and **2** together with OEP(Ni) are given in Figure 8. The electrochemical redox cycles of **1** and **2** were reversible and were analyzed to perform through two steps of one- and one-electron transfer processes toward the corresponding di-cationic species via radical-cations, similar to OEP(Ni), within a similar potential region to each other.[16]

In case of the reaction in 100% CH_2Cl_2 solution (Figure 8a), both **1** and **2** heightened their Ep_1 value by ca. 50 mV, as referred to that of OEP(Ni), and showed almost the same values between them. The Ep_1 values of referent compounds **22** and **23** are 960 and 900 mV, respectively, reflecting the orientation of DHBTh. This fact is the general case where an extension of π-electronic conjugation raises HOMO level of the molecule and thus lowers the Ep_1 value for the higher planar molecule **23** more intensively.[6b, 12] Taking this fact into consideration, the present behavior should be attributable to that an electronically inductive effect by the diacetylene-group connected DHBTh-Pyr constituent fully compensates for the extended π-

Table 2. The first oxidation potentials (E_{p1}/mV) of OEP-DHBTh-PAR and related compounds[1)]

OEP-DHBTh-PAR	CH_2Cl_2	HCO_2H		TFA
		10 eq.	10^3 eq.	10^3 eq.
OEP(Ni)	910	920	820	620
1	960	960	880	650
2	950	950	870	640
7	990			
8	1080			
22	960			
23	900			

1) Electrodes; GC (working), Pt (counter) and SCE (reference). Supporting electrolyte; *n*-Bu_4NClO_4. Scan rate; 120 mV/s. Each solution of the substrate in CH_2Cl_2 solution was adjusted to be 2.0 x 10^{-4} mol/cm^3.

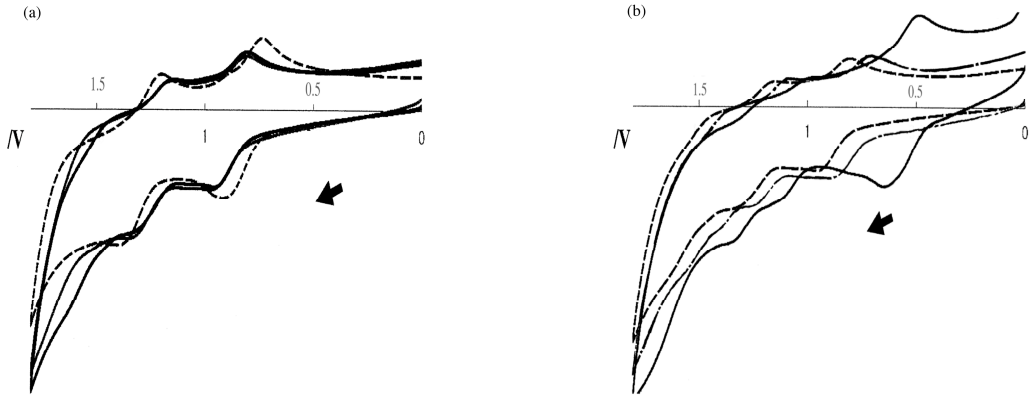

Figure 8. (a) shows cyclic voltammograms of **1** and **2** (solid line) together with OEP(Ni) (dashed line) in CH_2Cl_2 solution (25 ˚C). Voltammograms of **1** and **2** eventually almost overlapped. (b) shows cyclic voltammogram changes for **2** upon addition of 0 eq. molar amount of acid (dashed line), 10^3 eq. molar amount of HCO_2H (one-dot dashed line) and 10^3 eq. molar amount of TFA (solid line) into CH_2Cl_2 solution, respectively (see Table 2).

electronic conjugation effect with this residual constituent on OEP(Ni), lowering HOMO level of the OEP(Ni) ring in consequence. Especially in the case of **2**, it is suggested that an electron-withdrawing property of the Pyr ring is transmitted through the higher conjugation planarity of (TT)DHBTh toward the OEP(Ni) constituent more efficiently. In this respect, it is curious to compare these Ep_1 values with those of the OEP-DHBTh-(4)Pyr(NMe)I derivatives **7** and **8**, in which the DHBTh-(4)Pyr(NMe)I constituent behaves as much more electron-withdrawing substituent to OEP(Ni). Reflecting the orientation of DHBTh, the Ep_1 value of HH isomer **7** showed 990 mV and that of TT isomer **8** showed 1080 mV. This

result exactly indicates that an introduction of positive charge onto the Pyr constituent does not enhance their electron-releasing ability, but rather inductively lowers their HOMO level of the OEP(Ni) constituent with the greater magnitude for the more planar TT isomer.

On the other hand, when the electrochemical reactions were carried out in the presence of large excessive amount of acid, the derivatives **1** and **2** considerably lowered their E_{p_1} values, resulting in the enhanced electron-releasing ability under sufficiently acidic conditions. For example, the voltammograms of **2** under acidic conditions are shown in Figure 8b. In the case of formic acid (10^3 eq. molar amount of HCO_2H, *p*Ka 3.75),[17] both **1** and **2** lowered their E_{p_1} values by 80-90 mV, based on those in CH_2Cl_2. Surprisingly, the same 10^3 eq. molar amount of TFA exhibited further affection to lower their E_{p_1} values by more than 200 mV, based on the affection with HCO_2H. Under these acidic conditions, both **1** and **2** should be fully protonated onto the Pyr constituent, as shown in ^{1}H NMR spectral measurements. However, the structures under these conditions should be different from the ones simply protonated onto Pyr like **A'** (Scheme 4), because such simply positive-charged species would lower the HOMO level, *i.e.*, the poor electron-releasing ability, as seen in **7** and **8**. Moreover, it should be taken into consideration that OEP(Ni) itself also enhanced the electron-releasing ability under sufficiently acidic conditions (Table 2). Although the protonated structures of **1** and **2** under such acidic conditions are uncertain yet, a plausible feature of the structures will be discussed in the following section, based on all the spectral results obtained so far.

5. RELATIONSHIP OF SPECTRAL CHANGES WITH MOLECULAR STRUCTURES.

5. 1. SPECTRAL CHANGES IN THE FIRST STAGE. From ^{1}H NMR spectral, electronic absorption spectral, and electrochemical studies under the neutral and acidic conditions, it was revealed that the present OEP-DHBTh-PAR derivatives **1**-**6** behave in a unique system, reflecting the orientation of DHBTh, which is reversibly exchangeable between **A**-form and **A'**-form with TFA and NEt_3 (Scheme 4). It is no doubt that **A**-form corresponds to the neutral structure. Also, from the ^{1}H NMR spectral study, **A'**-form should correspond to the structure substantially protonated onto the PAR constituent in each derivative.

On one hand, from the electronic absorption spectral study, the serial spectra of **1**-**6** proved to change via two stages on adding acid. In the first stage, TFA (less than 10^4~10^5 eq. molar amount) mainly changed their intensities and shapes of Soret band, together with slightly intesifying Q band. In the second stage, TFA (more than ca. 10^5 eq. molar amounts) mainly changed their maxima of Q band to shift to the longer wavelength region. Both steady-state spectra should be brought from the protonated species on the PAR constituent, because the most proton-acceptable site in the molecule is PAR. The first steady-state spectra of **1** and **2**, for example, can be assigned to come from the purely protonated species **1'** and **2'**. Their

spectra were almost identical to the spectra of **7** and **8** bearing $^{(+)}$N-Me covalent bond (Figures 9a and 9b). It is also evident that TFA additive amount necessary for the first steady-state spectra were nearly the same between the respective HH and TT isomers in all pairs, regardless of the orientation of DHBTh. This fact apparently shows the protonation onto the lone-paired electrons of N atom in PAR, which are independent from the π-electronic conjugation of the extended system. Interestingly, acetic acid (AcOH, *p*Ka 4.76)[17] was found to be hard to protonate onto PAR of **1**-**4**, in spite of *p*Ka 5.20 well known for the conjugated acid Pyr-H^+,[18] indicating that the basicity of Pyr in the present extended conjugation system considerably weakens by an inductive effect of diacetylene linkage. HCO_2H (*p*Ka 3.75) protonated onto PAR of **1**-**4**, similar to TFA, to afford the definitely corresponding first steady-state spectra (Figures 9c and 9d), but could no longer change their spectra. No new Q band appeared in a longer wavelength region, even in 100% HCO_2H. As a primary conclusion in the first stage of acid addition experiment, it is indicated that *p*Ka values of the Pyr-H^+ site in **1**-**4** are somewhere between 3.75 of HCO_2H and 0.23 of TFA.

5. 2. SPECTRAL CHANGES IN THE SECOND STAGE. In the second stage of the electronic absorption spectral changes with TFA, it is suggested that the protonation onto the Pyr constituent produces some peculiar structural changes further into **1'**-**4'**, different from the simply positive-charged structures **A'** like **7** and **8**. The molecular structures responsible for the second steady-state spectra should be certainly the ones protonated onto PAR as well because of the more content of TFA in $CHCl_3$ solution, but must be different from the ones corresponding to the first steady-state spectra. As one of the candidates, the molecular structures in the second stage are tentatively predicted in the following. After protonation onto the PAR constituent in the first stage, an excessive amount of TFA seems to coordinate successively on the OEP(Ni) ring as an axial ligand. This ligandation of TFA on the OEP(Ni) ring weakens the back-donation interaction from Ni(II) to the 18π-electronic conjugation system of OEP, to pull its LUMO level down to some extent and oppositely to raise HOMO level up by a similar magnitude efficiently,[19] resulting in a longer wavelength shift of Q band by ca. 100 nm in electronic absorption spectra. Therefore, the ligandation of this type simultaneously results in an enhancement of the electron releasing ability as well. It is undoubted that the positive-charge introduced into PAR in the first stage also inductively weakens the coordination bonds of four N atoms of OEP with Ni(II) ion, leading to an acceleration of coordination of TFA on Ni(II) from the axial side concurrently (Figure 10).

In relation with the electronic absorption spectra, a peculiar ^{1}H NMR spectral phenomenon should not be ignored. Thus, the gradual peak-broadening phenomenon was observed only for the particular protons around the OEP(Ni) constituent of the molecule, immediately after saturation of the chemical shift changes of Pyr-H to the low field (Figure 4). Although it is not the same situation between ^{1}H NMR spectra, electronic absorption spectra, and CV experiments in concentration of the substrate in respective

solutions, the present peak-brpoadening phenomenon in their ^{1}H NMR spectra is rather likely related with the second stage in the electronic absorption spectral changes, especially with the Q band newly appearing in the longer wavelength region. In ^{1}H NMR spectra, the peak broadening phenomena of meso-H and methylene-H in the reference compounds **22**, **23**, and OEP(Ni) were not observed under the same conditions (1-5 eq. molar amount of TFA to the substrate in $CDCl_2CDCl_2$), but, to be surprised, were also gradually induced by adding more than ca. 75 eq. molar amount of TFA. This result apparently indicates that the protonation onto PAR in the first stage accelerates the peak broadening phenomenon of **1** and **2** with more than 30 times efficiency, as compared with that of OEP(Ni).

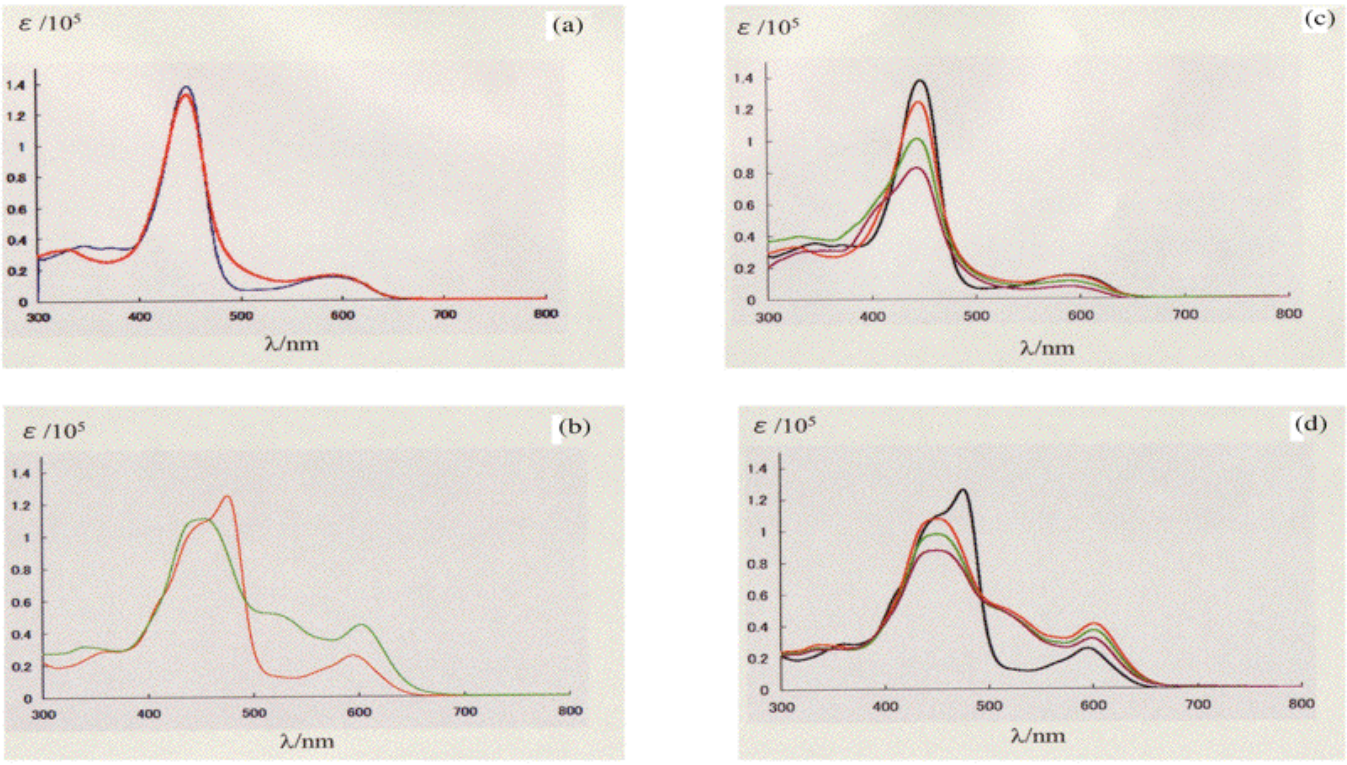

Figure 9. Electronic absorotion spectra. (a) **1** (blue line) and **7** (red line), (b) **2** (red line) and **8** (green line), (c) spectral changes of **1** with HCO_2H; for 0 eq. (black line), for 1.5 x 10^7 eq. (red line), for 2.0 x 10^7 eq. (green line), and for HCO_2H only (purple line), (d) spectral changes of **2** with HCO_2H; for 0 eq. (black line), for 1.5 x 10^7 eq. (red line), for 2.0 x 10^7 eq. (green line), and for HCO_2H only (purple line).

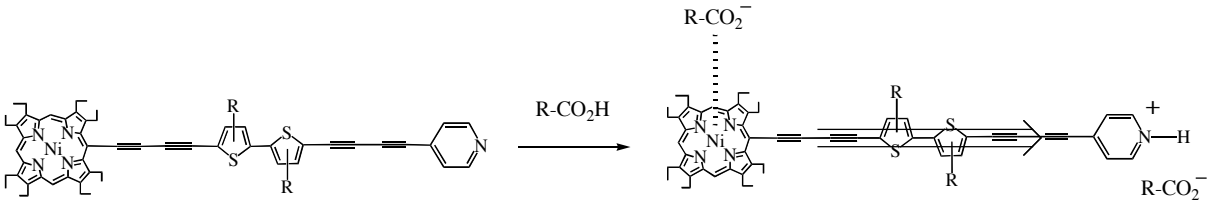

Figure 10. Protonated Pyr site works as a stronger electron-withdrawing group to OEP to weaken the coordination bond of four N atoms of OEP with Ni(II) ion and thus excessive amount of acid readily coordinates on Ni(II) ion as the fifth ligand.

5. 3. A TENTATIVE MECHANISM FOR PEAK BROADENING PHENOMENA IN ^{1}H NMR SPECTRA. There might be several reasons responsible for such peak broadening phenomena in ^{1}H NMR spectra. The coalescence between more than two conformational and/or geometrical isomers, however, would not necessarily be taken into account here in the metalloporphyrins such as **1** and **2**.[20] Face-to-face stacked aggregation of the OEP constituent is not the case, either, because no particular up-field shift of meso-H and other protons due to an anisotropic effect of the diamagnetic OEP(Ni) ring was observed.[21] In only a few cases of substituted porphyrin Ni(II) derivatives, it is known that paramagnetic complexes are formed upon addition of the axial ligands such as Pyr and piperidine.[22] The paramagnetism of this type undoubtedly induces the broadening of meso-H peaks, but simultaneously is accompanied by their pronounced up-field shifts. However, the formation of paramagnetic complex seemed to be uncertain in **1** and **2**, since a recognizable up-field shift of meso-H was not practically observed over the protonation experiments. Furthermore, addition of perdeuterated Pyr into a $CDCl_2CDCl_2$ solution of **2** did not change its spectrum so intensively as to be recognizable.

As derived from the electronic absorption spectral study, it may also be indicated from ^{1}H NMR spectral study that the protonation onto PAR with TFA accelerates coordination of excessive TFA as the fifth ligand on Ni(II) of the OEP constituent. This coordination would be simultaneously responsible for the peak broadening of meso-H. Based on the present experimental facts and predictions, the peak broadening phenomenon in ^{1}H NMR spectra is tentatively explained as follows. In a neutral medium, the three constituents of OEP(Ni), DHBTh, and PAR in the molecule should freely rotate along the molecular axis in such long one-dimensional skeletal system. Thus, all proton peaks appear in a very high resolution. This free rotation would continue until completion of protonation onto PAR. When an excessive amount of TFA starts coordinating on Ni(II) as an axial ligand after the protonation process, an activation energy for their free rotation would enlarge due to an increased bulkiness around OEP(Ni), resulting in an outstanding prolongation of the relaxation times for the particular protons around the OEP(Ni) constituent. Previously, it was proposed without any evidences that the TFA counter-anion migrates from Pyr-H^+ site to Ni(II) of OEP as a coordination ligand somehow.[4] It is rather reasonable to conclude that only the OEP(Ni) constituent coordinated with an excessive amount of TFA stops rotation in a solution at room temperature in consequence. On the other hand, it was found that the temperature elevation gradually recovered their peak sharpness and afforded the very high resolution spectra above 70 ˚C, with the chemical shifts completely remained (Figure 11). This evidence may support that such a bulky and crowded OEP(Ni) constituent again starts rotating along the molecular axis by overcoming an activation energy for desolvation, as summarized in Scheme 5. The present spectral behavior was also ascertained to be thermally reversible with high reproducibility.

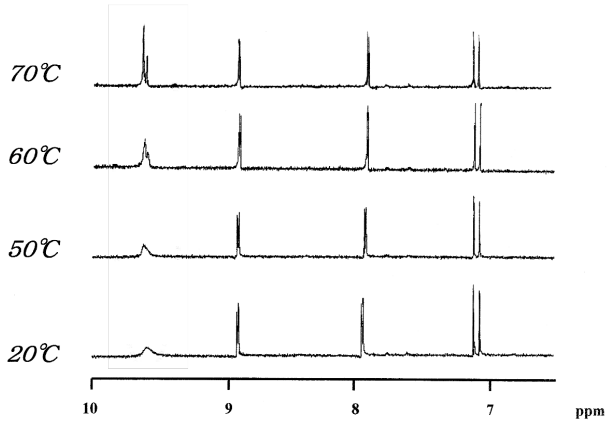

Figure 11. Variable temperature ^{1}H NMR spectra of **1** in a region between 7 ppm and 10 ppm ($CDCl_2CDCl_2$ containing 2.0 eq. molar amont of TFA to **1**, 600 MHz).

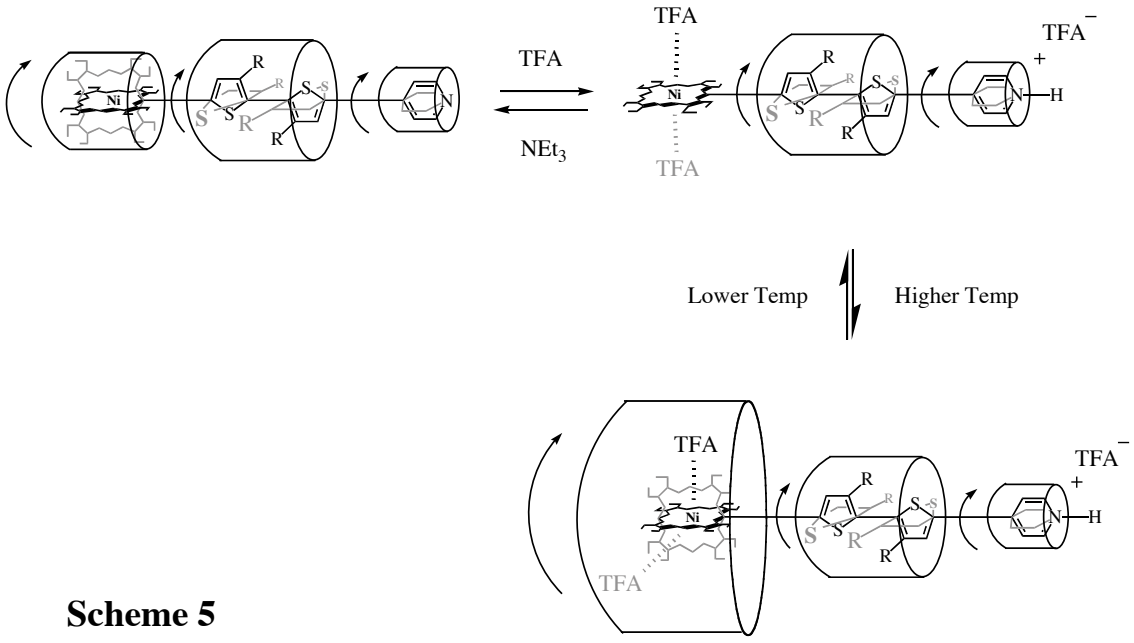

Scheme 5

CONCLUSIONS

Although a rational interpretation responsible for the peak broadening phenomenon in **1**-**6** should wait for further visual and quantitative studies,[23] the present extended OEP-DHBTh-PAR derivatives can be concluded to be a reversible system to show proton-mediated and heat-driven spectral changes. The structural and spectral conclusions in this study evidently come from the characteristic nature of the OEP-DHBTh-PAR molecular system, in which each constituent like a wheel of automobile is connected with the straight and rigid linkage of diacetylene like an axle of it. Further investigations of **1**-**8** under various conditions are still continuing.

EXPERIMETAL

The melting points were determined on a hot-stage apparatus and are uncorrected. IR spectra were measured on a Jasco FT/IR 7300 spectrophotometer as KBr disk or neat sample; only significant absorptions are reported. EI and FAB mass spectra were recorded with JEOL JMS-700 spectrometer. In case of the hard ionization by the above ionization techniques, ESI-FT-ICR mass spectra were performed with a Bruker BioAPEX 70e spectrometer equipped with a 7T superconducting magnet, using a sample in a solution of $CHCl_3$:MeOH. ^1H NMR spectra were measured in $CDCl_3$ and/or $CDCl_2CDCl_2$ and/or THF-d_8 solutions on a JEOL JMN-EPC 600 (600 MHz) spectrometer and were recorded in δ values (/ppm) with TMS as an internal standard. The coupling constants (*J*) are given in Hz. Electronic absorption spectra were measured in $CHCl_3$ solution on a Shimadzu UV-2200A spectrophotometer (sh=shoulder), unless otherwise stated. The measurement of oxidation potentials with CV was performed on a BAS CV-27 potentiometer in CH_2Cl_2 in the presence of *n*-Bu_4NClO_4 at a scan rate of 120 mV/s. SiO_2 (Fujisilysia BW 820MH or BW 127ZH) and aluminum oxide (Al_2O_3, CAMAG 504-C-1) were used for column chromatography. Reactions were followed by TLC aluminum sheets precoated with Merck SiO_2 F_{254} or with Merck Al_2O_3 GF_{254}. Organic extracts were dried over anhydrous sodium sulfate (Na_2SO_4) or magnesium sulfate ($MgSO_4$) prior to removal of the solvents.

OEP(Ni)-(HH)DHBTh-(4)Pyr (1): A solution of the terminal acetylenes of **9**[6] (132 mg, 0.13 mmol) and **11**[7] (200 mg, 1.43 mmol) in Pyr and MeOH (200 cm^3, 5:1) was added to a mixed solution of Pyr and MeOH (80 cm^3, 5:1) containing anhydrous copper(II) acetate ($Cu(OAc)_2$, 600 mg, 3.3 mmol) under Ar atmosphere at 40 ˚C over 12 h. After stirred at 40 ˚C for additional 6 h, the mixture was poured into water and extracted with $CHCl_3$. The extracts were washed with brine several times and dried. After removal of low-boiling solvents such as $CHCl_3$ and MeOH and of Pyr under reduced pressure successively, the residue was chromatographed on Al_2O_3 (ϕ 4.2 x 15 cm) with hexane-$CHCl_3$ (1:1) to afford **1** (80 mg, 55%) from the first fractions and the dicaetylene-group connected Pyr dimer **14**[8] (66 mg) and the OEP-(HH)DHBTh homo-coupling dimer **15**[9] (4 mg) from the following fractions. **1**: black purple fine crystals ($CHCl_3$-MeOH); Mp >285 ˚C (gradual decomp); Mass (MALDI TOF) m/z 1096.4 (M^++1) for $C_{69}H_{75}N_5S_2Ni$, MW=1095.4; IR (KBr) 2962, 2927 and 2869 (CH) and 2200 and 2130 cm^{-1} (C:::C); ^1H NMR ($CDCl_3$) δ=9.42 (2H, s, meso-H), 9.39 (1H, s, meso-H), 8.61 (2H, d, *J*=4, Pyr-H2 and H6), 7.36 (2H, d, *J*=4, Pyr-H3 and H5), 4.12 (4H, q, *J*=8, C*H*$_2$-CH_3), 3.81-3.77 (12H, m, C*H*$_2$-CH_3), 2.52 (4H, br t, *J*=8, C*H*$_2$-$(CH_2)_4CH_3$), 1.81-1.71 (24H, m, CH_2-C*H*$_3$), 1.28-1.26 (16H, m, CH_2-(C*H*$_2$)$_4CH_3$), 0.90-0.87 (6H, m, CH_2-$(CH_2)_4$C*H*$_3$); UV-VIS ($CHCl_3$) λ_{max}=347 (ε 35700), 449 (138000) and 589 nm (14800). Anal. Calcd for $C_{69}H_{75}N_5S_2Ni$: C, 75.53; H, 6.89; N, 6.38%. Found: C, 75.48; H, 6.95; N, 6.33%. **14**[8]: colorless powder; Mass (EI) m/z 204 (M^+) for $C_{14}H_8N_2$, MW=204.23; IR (KBr) 1940 and 1915 cm^{-1} (C:::C); ^1H NMR ($CDCl_3$) δ=8.65 (4H, d, *J*=4, Pyr-H2 and H6) and 7.39 (4H, d, *J*=4, Pyr-H3 and H5); UV-VIS

($CHCl_3$) λ_{max}=290 (ε 3000), 310 (3980) and 330 (3530). **15**[9]: IR (KBr) 2961, 2925 and 2869 (CH) and 2155 and 2125 cm^{-1} (C:::C); ^1H NMR (THF-d_8) δ=9.48 (4H, s, meso-H), 9.46 (2H, s, meso-H), 7.44 (2H, s, Th-H), 7.37 (2H, s, Th-H), 4.16 (8H, q, *J*=6.6, OEP-CH_2), 3.86-3.77 (24H, m, CH_2-CH_3), 2.55-2.50 (8H, br m, CH_2-$(CH_2)_4CH_3$), 1.86-1.20 (80H, m, CH_2-CH_3 and CH_2-(CH_2)$_4CH_3$), 0.90-0.87 (12H, t m, CH_2-$(CH_2)_4$CH_3).

OEP(Ni)-(TT)DHBTh-(4)Pyr (2): The derivative **2** was synthesized from **10**[6] (180 mg, 0.18 mmol) and **11**[7] (250 mg, 1.8 mmol) by the same way and processes as for **1**. **2:** Yiled; 71%; black purple fine crystallines ($CHCl_3$-MeOH); Mp >280 ˚C (gradual decomp); Mass (MALDI TOF) m/z 1096.5 (M^++1) for $C_{69}H_{75}N_5S_2Ni$, MW=1095.4; IR (KBr) 2959, 2924 and 2851 (CH) and 2196 and 2122 cm^{-1} (C:::C); ^1H NMR ($CDCl_3$) δ=9.42 (2H, s, meso-H), 9.39 (1H, s, meso-H), 8.62 (2H, d, *J*=4, Pyr-H2 and H6), 7.37 (2H, d, *J*=4, Pyr-H3 and H5), 4.13 (4H, q, *J*=8, CH_2-CH_3), 3.83-3.76 (12H, m, CH_2-CH_3), 2.77 (2H, t, *J*=8, CH_2-$(CH_2)_4CH_3$), 2.70 (2H, t, *J*=8, CH_2-$(CH_2)_4CH_3$), 1.81-1.71 (24H, m, CH_2-CH_3), 1.37-1.33 (16H, m, CH_2-(CH_2)$_4CH_3$), 0.92-0.87 (6H, m, CH_2-$(CH_2)_4$CH_3); UV-VIS ($CHCl_3$) λ_{max}=350 (ε 27000, sh), 445 (105000, sh), 476 (125000) and 594 nm (25000). Anal. Calcd for $C_{69}H_{75}N_5S_2Ni$: C, 75.53; H, 6.89; N, 6.38%. Found: C, 75.63; H, 6.99; N, 6.41%. The later fractions afforded **14** (52 mg) and the OEP-(TT)DHBTh homo-coupling dimer **16** (6 mg). **16**[9]: IR (KBr) 2961, 2925 and 2869 (CH) and 2147 and 2123 cm^{-1} (C:::C); ^1H NMR (THF-d_8) δ=9.51 (4H, s, meso-H), 9.48 (2H, s, meso-H), 7.24 (2H, s, Th-H), 7.21 (2H, s, Th-H), 4.18 (8H, q, *J*=6.6, OEP-CH_2), 3.90-3.80 (24H, m, CH_2-CH_3), 2.85 (4H, t, *J*=7.6, CH_2-$(CH_2)_4CH_3$), 2.75 (4H, t, *J*=7.5, CH_2-$(CH_2)_4CH_3$), 1.86-1.28 (80H, m, CH_2-CH_3 and CH_2-(CH_2)$_4CH_3$), 0.95-0.89 (12H, t m, CH_2-$(CH_2)_4$CH_3).

OEP(Ni)-(HH)DHBTh-(2)Pyr (3): A solution of the terminal acetylenes of **9**[6] (65 mg, 0.063 mmol) and **12**[7] (110 mg, 1.07 mmol) in Pyr (100 cm^3) was added into Pyr (60 cm^3) containing $Cu(OAc)_2$ (400 mg, 2.2 mmol) under Ar atmosphere at 40 ˚C over 12 h. After stirred at 40 ˚C for additional 6 h, the mixture was poured into water and extracted with $CHCl_3$. The extracts were washed with brine several times and dried. After removal of low-boiling solvents such as $CHCl_3$ and MeOH and of Pyr under reduced pressure successively, the residue was chromatographed on Al_2O_3 (ϕ 1.5 x 40 cm) with hexane-$CHCl_3$ (7:3) to afford **3** (40 mg, 58%), together with **15** (4 mg). Isolation of the homo-coupling dimer corresponding to **14** was given up due to hard separation from the mixture. **3**: black purple fine crystals ($CHCl_3$-MeOH); Mp >285 ˚C (gradual decomp); Mass (MALDI TOF) m/z 1096.4 (M^++1) for $C_{69}H_{75}N_5S_2Ni$, MW=1095.4; IR (KBr) 2961, 2926 and 2867 (CH) and 2202 and 2129 cm^{-1} (C:::C); ^1H NMR ($CDCl_3$) δ=9.42 (2H, s, meso-H), 9.39 (1H, s, meso-H), 8.62 (1H, dd, *J*=5 and 1, Pyr-H6), 7.66 (1H, dt, *J*=8 and 5, H4), 7.52 (1H, dd, *J*=8 and 1, H3), 7.28 (1H, s, Th-H), 7.27 (1H, dt, *J*=8 and 5, H5), 7.26 (1H, s, Th-H), 4.12 (4H, q, *J*=8, CH_2-CH_3), 3.81-3.76 (12H, m, CH_2-CH_3), 2.52 (4H, br t, *J*=8, CH_2-$(CH_2)_4CH_3$), 1.81-1.71 (24H, m, CH_2-CH_3), 1.28-1.25 (16H, m, CH_2-(CH_2)$_4CH_3$), 0.90-0.87 (6H, m, CH_2-$(CH_2)_4$CH_3); UV-VIS ($CHCl_3$)

λ_{max}=344 (ε 37000), 449 (141000) and 590 nm (14700). Anal. Calcd for $C_{69}H_{75}N_5S_2Ni$: C, 75.53; H, 6.89; N, 6.38%. Found: C, 75.40; H, 7.05; N, 6.29%.

OEP(Ni)-(TT)DHBTh-(2)Pyr (4): The derivative **4** was synthesized from **10**[6] (62 mg, 0.06 mmol) and **12**[7] (100 mg, 0.97 mmol) by the same way and procedures as for **3**. **4:** Yield 60%; black purple fine crystals ($CHCl_3$-MeOH); Mp >280 °C (gradual decomp); Mass (MALDI TOF) m/z 1096.5 (M^++1) for $C_{69}H_{75}N_5S_2Ni$, MW=1095.4; IR (KBr) 2962, 2927 and 2867 (CH) and 2198 and 2127 cm^{-1} (C:::C); ^1H NMR ($CDCl_3$) δ=9.42 (2H, s, meso-H), 9.39 (1H, s, meso-H), 8.62 (1H, dd, *J*=5 and 1, Pyr-H6), 7.66 (1H, dt, *J*=8 and 5, H4), 7.52 (1H, dd, *J*=8 and 1, H3), 7.27 (1H, dt, *J*=8 and 5, H5), 6.99 (1H, s, Th-H), 6.96 (1H, s, Th-H), 4.13 (4H, q, *J*=8, C*H*$_2$-CH_3), 3.81-3.77 (12H, m, C*H*$_2$-CH_3), 2.77 (4H, t, *J*=8, C*H*$_2$-$(CH_2)_4CH_3$), 2.70 (4H, t, *J*=8, C*H*$_2$-$(CH_2)_4CH_3$), 1.81-1.71 (24H, m, CH_2-C*H*$_3$), 1.37-1.33 (16H, m, CH_2(C*H*$_2$)$_4CH_3$), 0.92-0.88 (6H, m, CH_2-$(CH_2)_4$C*H*$_3$); UV-VIS ($CHCl_3$) λ_{max}=350 (ε 24000), 445 (91000), 476 (107000) and 594 nm (22000). Anal. Calcd for $C_{69}H_{75}N_5S_2Ni$: C, 75.53; H, 6.89; N, 6.38%. Found: C, 75.61; H, 7.12; N, 6.36%. The reaction also gave the homo-coupling product **16**[9] (3 mg).

When this reaction was carried out in a mixed solvent of Pyr with MeOH (1:1), the derivative **4** was not obtained at all. Instead, the MeOH-participated derivatives **17** and **18** were isolated together with **16**[9] (8%), after the same work-up and procedures. **17:** Yield 27% based on **10**; black purple microcrystallines; Mp >280 °C (gradual decomp); Mass (MALDI TOF) m/z 1049.4 (M^++1) for $C_{65}H_{74}N_4OS_2Ni$, MW=1048.4; IR (KBr) 2962, 2927 and 2872 (CH) and 2178 and 2128 cm^{-1} (C:::C); ^1H NMR ($CDCl_3$) δ=9.40 (2H, s, meso-H), 9.37 (1H, s, meso-H), 7.04 (1H, s, Th-H), 7.01 (1H, s, Th-H), 4.10 (4H, q, *J*=8, C*H*$_2$-CH_3), 3.84 (3H, s, Me-H), 3.79-3.73 (12H, m, C*H*$_2$-CH_3), 2.94 (2H, t, *J*=8, C*H*$_2$-$(CH_2)_4CH_3$), 2.75 (2H, t, *J*=8, C*H*$_2$-$(CH_2)_4CH_3$), 1.78-1.69 (24H, m, CH_2-C*H*$_3$), 1.34-1.28 (16H, m, CH_2(C*H*$_2$)$_4CH_3$), 0.87-0.84 (6H, m, CH_2-$(CH_2)_4$C*H*$_3$); UV-VIS ($CHCl_3$) λ_{max}=345 (ε 20000), 442 (78000), 467 (91000) and 592 nm (16000). Anal. Calcd for $C_{65}H_{74}N_4OS_2Ni$: C, 74.34; H, 7.10; N, 5.33%. Found: C, 74.08; H, 7.40; N, 5.22%. **18:** Yield 35% based on **10**; black purple microcrystals; Mp 265-270 °C (decomp); Mass (MALDI TOF) m/z 1128.5 (M^++1) for $C_{70}H_{79}N_5OS_2Ni$, MW=1127.5; IR (KBr) 2962, 2927 and 2868 (CH) and 2166 and 2126 cm^{-1} (C:::C); ^1H NMR ($CDCl_3$) δ=9.42 (2H, s, meso-H), 9.39 (1H, s, meso-H), 8.55 (1H, dd, *J*=5 and 1, Pyr-H6), 7.70 (1H, dt, *J*=8 and 5, H4), 7.66 (1H, dd, *J*=8 and 1, H3), 7.23 (1H, dt, *J*=8 and 5, H5), 6.98 (1H, s, Th-H), 6.96 (1H, s, Th-H), 6.61 (1H, s, olefinic-H), 4.32 (3H, s, Me-H), 4.13 (4H, q, *J*=8, C*H*$_2$-CH_3), 3.81-3.76 (12H, m, C*H*$_2$-CH_3), 2.77 (2H, t, *J*=8, C*H*$_2$-$(CH_2)_4CH_3$), 2.67 (2H, t, *J*=8, C*H*$_2$-$(CH_2)_4CH_3$), 1.81-1.72 (24H, m, CH_2-C*H*$_3$), 1.36-1.33 (16H, m, CH_2(C*H*$_2$)$_4CH_3$), 0.91-0.87 (6H, m, CH_2-$(CH_2)_4$C*H*$_3$); UV-VIS ($CHCl_3$) λ_{max}=368 (ε 26000), 446 (91000), 475 (107000) and 595 nm (22000). Anal. Calcd for $C_{70}H_{79}N_5OS_2Ni$: C, 74.45; H, 7.05; N, 6.20%. Found: C, 74.18; H, 7.33; N, 6.11%.

OEP(Ni)-(HH)DHBTh-(2)Pym (5): A solution of the terminal acetylenes of **9**[6] (14 mg, 0.014 mmol) and

13 (40 mg, 0.38 mmol) in Pyr (40 cm^3) was added into Pyr (40 cm^3) containing $Cu(OAc)_2$ (200 mg, 1.1 mmol) under Ar atmosphere at 40 ˚C over 12 h. After stirred at 40 ˚C for additional 6 h, the mixture was poured into water and extracted with $CHCl_3$. The extracts were washed with brine several times and dried. After removal of low-boiling solvents such as $CHCl_3$ and MeOH and of Pyr under reduced pressure successively, the residue was chromatographed on Al_2O_3 (ϕ 1.5 x 40 cm) with hexane-$CHCl_3$ (7:3) to afford **3** (8 mg, 52%), together with **15**[9] (1 mg). Isolation of the homo-coupling dimer corresponding to **14** was given up due to hard separation from the mixture. **5**: black purple fine crystallines ($CHCl_3$-MeOH); Mp >280 ˚C (gradual decomp); Mass (MALDI TOF) m/z 1097.5 (M^++1) for $C_{68}H_{74}N_6S_2Ni$, MW=1096.4; IR (KBr) 2965, 2929 and 2870 (CH) and 2210 and 2132 cm^{-1} (C:::C); ^{1}H NMR ($CDCl_3$) δ=9.42 (2H, s, meso-H), 9.39 (1H, s, meso-H), 8.74 (2H, d, *J*=5, Pyr-H4 and H6), 7.28 (1H, t, *J*=5, H5), 7.26 (1H, s, Th-H), 7.24 (1H, s, Th-H), 4.12 (4H, q, *J*=8, C*H*$_2$-CH_3), 3.82-3.77 (12H, m, C*H*$_2$-CH_3), 2.53-2.50 (4H, tm, C*H*$_2$-$(CH_2)_4CH_3$), 1.81-1.71 (24H, m, CH_2-C*H*$_3$), 1.29-1.25 (16H, m, CH_2-(C*H*$_2$)$_4CH_3$), 0.89-0.87 (6H, m, CH_2-$(CH_2)_4$C*H*$_3$); UV-VIS ($CHCl_3$) λ_{max}=339 (ε 35000), 448 (140000) and 591 nm (35000). Anal. Calcd for $C_{68}H_{74}N_6S_2Ni$: C, 74.38; H, 6.79; N, 7.66%. Found: C, 74.30; H, 7.05; N, 7.55%.

OEP(Ni)-(TT)DHBTh-(2)Pym (6): The derivative **6** was synthesized from **10**[6] (22 mg, 0.02 mmol) and **13** (50 mg, 0.48 mmol) by the same way and procedures as for **5**. **6**: Yield 38%; black purple fine crystals ($CHCl_3$-MeOH); Mp >280 ˚C (gradual decomp); Mass (MALDI TOF) m/z 1097.5 (M^++1) for $C_{68}H_{74}N_6S_2Ni$, MW=1096.4; IR (KBr) 2963, 2928 and 2869 (CH) and 2202 and 2132 cm^{-1} (C:::C); ^{1}H NMR ($CDCl_3$) δ=9.42 (2H, s, meso-H), 9.39 (1H, s, meso-H), 8.75 (2H, d, *J*=5, Pyr-H4 and H6), 7.27 (1H, t, *J*=5, H5), 7.02 (1H, s, Th-H), 6.98 (1H, s, Th-H), 4.13 (4H, q, *J*=8, C*H*$_2$-CH_3), 3.81-3.77 (12H, m, C*H*$_2$-CH_3), 2.78 (2H, t, *J*=8, C*H*$_2$-$(CH_2)_4CH_3$), 2.71 (2H, t, *J*=8, C*H*$_2$-$(CH_2)_4CH_3$), 1.81-1.72 (24H, m, CH_2-C*H*$_3$), 1.36-1.33 (16H, m, CH_2-(C*H*$_2$)$_4CH_3$), 0.92-0.88 (6H, m, CH_2-$(CH_2)_4$C*H*$_3$); UV-VIS ($CHCl_3$) λ_{max}=350 (ε 25000), 449 (100000), 477 (114000) and 595 nm (25000). Anal. Calcd for $C_{68}H_{74}N_6S_2Ni$: C, 74.38; H, 6.79; N, 7.66%. Found: C, 74.18; H, 6.88; N, 7.58%. The reaction also gave **16**[9] (1 mg).

OEP(Ni)-(HH)DHBTh-(4)Pyr(MeI) (7): A mixture of **1** (4 mg, 3.64 x 10^{-3} mmol) and MeI (0.3 cm^3, 4.82 mmol) in Ar-purged acetone (5 cm^3) in a sealed tube was refluxed gently overnight. After removal of the solvent, the reaction mixture was recrystallized from hexane-$CHCl_3$ to afford **7** (4.5 mg, quantitative) as black purple microcrystallines. Mp >250 ˚C (gradual decomp); Mass (MALDI TOF) m/z 1110.5 (M^+-127) for $C_{70}H_{78}N_5S_2NiI$, MW=1237.4; IR (KBr) 2963, 2928 and 2869 (CH) and 2191 and 2128 cm^{-1} (C:::C); ^{1}H NMR ($CDCl_3$) δ=9.44 (2H, s, meso-H), 9.42 (1H, s, meso-H), 8.38 (2H, d, *J*=6, Pyr-H2 and H6), 7.39 (1H, s, Th-H), 7.34 (2H, d, *J*=6, Pyr-H3 and H5), 7.31 (1H, s, Th-H), 4.13 (4H, q, *J*=8, C*H*$_2$-CH_3), 3.96 (3H, s, Me-H), 3.83-3.72 (12H, m, C*H*$_2$-CH_3), 2.54 (4H, br t, *J*=8, C*H*$_2$-$(CH_2)_4CH_3$), 1.82-1.72 (24H, m, CH_2-C*H*$_3$), 1.31-1.25 (16H, m, CH_2-(C*H*$_2$)$_4CH_3$), 0.90-0.87 (6H, m, CH_2-$(CH_2)_4$C*H*$_3$);

UV-VIS ($CHCl_3$) λ_{max}=329 (ε 33000), 447 (133000) and 589 nm (16000). Anal. Calcd for $C_{70}H_{78}N_5S_2NiI$: C, 75.59; H, 7.07; N, 6.30%. Found: C, 75.33; H, 7.10; N, 6.15%.

OEP(Ni)-(TT)DHBTh-(4)Pyr(MeI) (8): The derivative **8** was synthesized from **2** (3 mg, 2.37 x 10^{-3} mmol) and MeI (0.2 cm^3, 3.21 mmol) by the same way and procedures as for **7**. **8:** Yield 98%; black purple microcrystals (hexane-$CHCl_3$); Mp >250 ˚C (gradual decomp); Mass (MALDI TOF) m/z 1110.5 (M^+-127) for $C_{70}H_{78}N_5S_2NiI$, MW=1237.4; IR (KBr) 2961, 2926 and 2868 (CH) and 2180 and 2123 cm^{-1} (C:::C); ^{1}H NMR ($CDCl_3$) δ=9.45 (2H, s, meso-H), 9.43 (1H, s, meso-H), 7.64 (2H, d, *J*=6, Pyr-H2 and H6), 6.96 (1H, s, Th-H), 6.93 (1H, s, Th-H), 6.84 (2H, d, *J*=6, Pyr-H3 and H5), 4.15 (4H, q, *J*=8, C*H*$_2$-CH_3), 3.84-3.79 (12H, m, C*H*$_2$-CH_3), 3.25 (3H, s, Me-H), 2.76 (4H, br t, *J*=8, C*H*$_2$-$(CH_2)_4CH_3$), 1.82-1.69 (24H, m, CH_2-C*H*$_3$), 1.38-1.25 (16H, m, CH_2-(C*H*$_2$)$_4CH_3$), 0.98-0.88 (6H, m, CH_2-$(CH_2)_4$C*H*$_3$); UV-VIS ($CHCl_3$) λ_{max}=334 (ε 33000), 454 (111000) 521 (51000) and 602 nm (44000). Anal. Calcd for $C_{70}H_{78}N_5S_2NiI$: C, 75.59; H, 7.07; N, 6.30%. Found: C, 75.41; H, 7.33; N, 6.00%.

2-Ethynylpyrimidine (13): A solution of 2-bromopyrimidine[7] (1.2 g, 7.55 mmol) and trimethylsilylacetylene (1.5 cm^3, 10.6 mmol) containing copper(I) iodide (20 mg, 0.11 mmol) and dichlorobis(triphenylphisphine)palladium (200 mg, 0.28 mmol) in diisopropylamine (20 cm^3) was stirred over 10 h at an ambient temperature. Poured into water, the reaction mixture was extracted with $CHCl_3$, washed with brine and then dried. The resdiue obtained after removal of the solvent was chromatographed on Al_2O_3 (ϕ 2.1 x 7 cm) with hexane to afford 2-(trimethylsilylethynyl)pyrimidine: Yield 98%; pale yellow solid; Mass (EI) m/z 176 (M^+) for $C_9H_{12}Si_2N_2$, MW=176; IR (KBr) 2968 and 2900 (CH) and 2067 cm^{-1} (C:::C); ^{1}H NMR ($CDCl_3$) δ=8.72 (2H, d, *J*=5, Pym-H), 7.25 (1H, t, *J*=5, Pym-H), 0.30 (9H, s, $SiCH_3$); UV-VIS ($CHCl_3$) λ_{max}=242 (ε 12000). Anal. Calcd for $C_9H_{12}Si_2N_2$: C, 61.32; H, 6.86; N, 15.89%. Found: C, 61.15; H, 7.08; N, 15.77%. A solution of the trimethylsilylethynylpyrimidine (700 mg, 3.97 mmol) and anhydrous potassium carbonate (K_2CO_3; 100 mg, 0.72 mmol)[6b] in a mixture of MeOH and $CHCl_3$ (12 cm^3, 1:1) was stirred under Ar atmosphere over 4 h. Poured into water, the reaction mixture was extracted with $CHCl_3$, washed with brine and then dried. The residue obtained after removal of the solvent was chromatographed on Al_2O_3 (ϕ 2.1 x 1 cm) with $CHCl_3$ to afford **13** (280 mg, 68%) as pale yellow solid. Mass (EI) m/z 104 (M^+) for $C_6H_4N_2$, MW=104; IR (KBr) 3250 (C:::CH) and 2120 cm^{-1} (C:::C); ^{1}H NMR ($CDCl_3$) δ=8.75 (2H, d, *J*=5, Pym-H), 7.30 (1H, t, *J*=5, Pym-H), 3.17 (1H, s, C:::CH); UV-VIS ($CHCl_3$) λ_{max}=240 (ε 10000). Anal. Calcd for $C_6H_4N_2$: C, 69.21; H, 3.87; N, 26.91%. Found: C, 69.00; H, 3.95; N, 26.88%.

ACKNOWLEDGMENT

Financial support by a Grant-in-Aid for Scientific Research from the Ministry of Education, Science, Sports, Culture and Technology, is gratefully acknowledged. The present work was financially supported

in part by The Hokuriku Industrial Advancement Center (HIAC). HH is also grateful to VBL Research Center and Center of Instrumental Analyses at University of Toyama for their supporting measurements of physical properties of the new compounds.

REFERENCES AND NOTES

1. (a) T. Ema, N. Ouchi, T. Doi, T. Korenaga, and T. Sakai, *Org. Lett.*, 2005, **7**, 3985. (b) M. J. Frampton, H. Akdas, A. R. Cowley, J. E. Rogers, J. E. Slagle, P. A. Fleitz, M. Drobizhev, A. Rebane, and H. L. Anderson, *Org. Lett.*, 2005, **7**, 5365. (c) G. Kodis, Y. Terazono, P. A. Liddle, J. Andresson, V. Garg, M. Hambourger, T. A. Moore, A. L. Moore, and D. Gust, *J. Am. Chem. Soc.*, 2006, **128**, 1818. (d) A. Gabrielsson, F. Hartl, H. Zhang, J. R. L. Smith, M. Towrie, A. Vlcek, Jr., and R. N. Perutz, *J. Am. Chem. Soc.*, 2006, **128**, 4253. (e) Y. Ishii, Y. Onda, and Y. Kubo, *Tetrahedron Lett.*, 2006, **47**, 8221. (f) Y. Li, Z. Gan, N. Wang, X. He, Y. Li, S. Wang, H. Liu, Y. Araki, O. Ito, and D. Zhu, *Tetrahedron*, 2006, **62**, 4285. (g) H. Ozawa, M. Kawano, H. Tanaka, and T. Ogawa, *Tetrahedron*, 2006, **62**, 4749. (h) A. J. F. N. Sobral, S. M. Melo, M. L. Romas, R. Teixeira, S. M. Andrade, and S. M. B. Coata, *Tetrahedron Lett.*, 2007, **48**, 3145. (i) X. Liu, J. Liu, J. Pan, S. Andersson, and L. Sun, *Tetrahedron*, 2007, **63**, 9195. (j) J. Wu, F. Fang, W. -Y. Lu, J. –L. Hou, C. Li, Z. –Q. Wu, X. –K. Jiang, Z. –T. Li, and Y. Yu, *J. Org. Chem.*, 2007, **72**, 2897.
2. (a) T. Yamamura, A. Momotake, and T. Arai, *Tetrahedron Lett.*, 2004, **45**, 9219. (b) S. D. Straight, J. Andresson, G. Kodis, S. Bnadyopadhyay, R. H. Mitchell, T. A. Moore, A. L. Moore, and D. Gust, *J. Am. Chem. Soc.*, 2005, **127**, 9403 and many other references.
3. (a) Z. –Q. Wu, X. –B. Shao, C. Li, J. –L. Hou, K. Wang, X. –K. Jiang, and Z. –T. Li, *J. Am. Chem. Soc.*, 2005, **127**, 17460. (b) T. Muraoka, K. Kinbara, and T. Aida, *Nature*, 2006, **440**, 512. (c) P. Bhyrappa, V. V. Borovkov, and Y. Inoue, *Org. Lett.*, 2007, **9**, 433 and many other references.
4. A part of the present works was preliminarily reported; N. Hayashi, T. Matsukihira, K. Miyabayashi, M. Miyake, and H. Higuchi, *Tertahedron Lett.*, 2006, **47**, 5585.
5. G. Eglinton and A. R. Galbraith, *Chem. Ind.*, 1956, 737. Under the original Eglinton conditions,oxidative coupling reactions were carried out in the presence of large excesive amount of copper(II) monohydrate in either Pyr, dimethylformamide (DMF), or morpholine.
6. N. Hayashi, A. Matsuda, E. Chikamatsu, K. Mori, and H. Higuchi, *Tetrahedron Lett.*, 2003, **44**, 7155. (b) N. Hayashi, M. Murayama, K. Mori, A. Matsuda, E. Chikamatsu, K. Tani, M. Miyake, and H. Higuchi, *Tetrahedron*, 2004, **60**, 6363.
7. Purchased from Sigma-Aldrich Fine Chemicals Co., Ltd., Product No. 530921-1 for **11**, No. 469920-1 for **12** and No. 4595-60-2 for 2-bromopyrimidine.
8. L. D. Ciana and A. Haim, *J. Heterocycl. Chem.*, 1984, **21**, 607.
9. (a) H. Higuchi, H. Yamamoto, J. Ojima, and G. Yamamoto, *J. Chem. Soc., Perkin Trans.* 1, 1993, 975. (b) H. Higuchi, H. Yamamoto, J. Ojima, and G. Yamamoto, *Bull. Chem. Soc. Jpn.*, 1993, **66**, 2323. (c) H. Imahori, H. Higuchi, Y. Matsuda, A. Itagaki, Y. Sakai, J. Ojima, and Y. Sakata, *Bull. Chem. Soc. Jpn.*, 1994, **67**, 2500 and others cited therein.
10. H. Higuchi, T. Ishikura, K. Mori, Y. Takayama, K. Yamamoto, K. Tani, K. Miyabayashi, and M. Miyake, *Bull. Chem. Soc. Jpn.*, 2001, **74**, 889.
11. N. Hayashi, A. Naoe, K. Miyabayashi, M. Miyake, and H. Higuchi, *Tetraheron Lett.*, 2005, **46**, 6961.
12. N. Hayashi, H. Nishi, K. Morizumi, I. Kobayashi, H. Sakai, R. Akaike, K. Tani, and H. Higuchi, In *Recent Research Developments in Organic Chemistry*, ed. by S. G. Pandalai, Transworld Research Network (Kerala), 2004, Vol. 8, 401.
13. Related reactions with the present MeOH addition to **4** for generality are further investigated, as well as X-ray structure analysis of **18**.

14. H. C. Brown, D. H. McDaniel, and O. Haflinger, In *Determination of Organic Structures by Physical Methods*, ed. by E. A. Braude and F. C. Nachod, Acadmic Press (New York), 1955, Chapter 14.
15. Electrochemical properties of **1**-**8** will be reported conclusively, from the viewpoint of acid-, temparature-, concentration- and solvent-dependences.
16. (a) J. –H. Fuhrhop, K. M. Kaddish, and D. G. Davis, *J. Am. Chem. Soc*., 1973, **95**, 5140. (b) J. –H. Fuhrhop, In *Porphyrins and Metalloporphyrins*, ed. by K. M. Smith, Elsevier Scientific Publishing Co. (New York), 1975, Sec. F, Chapter 14.
17. G. H. Mansfield and M. C. Whiting, *J. Chem. Soc*., 1956, 4761.
18. D. M. Smith, In *Rodd's Chemistry of Carbon Compounds*, ed. by S. Coffey, 2nd. Edition, Elsevier (Amsterdam), 1976, Vol. IV^F.
19. J. W. Buchler, In *The Porphyrins*, ed. by D. Dolphin, Academic Press (New York), 1978, Vol. Chapter 10.
20. H. Scheer and J. J. Katz, In *The Porphyrins and Metalloporphyrins*, ed. by K. M. Smith, Elsevier Scientific Publishing (New York), 1975, Vol. III, Chapter 10; T. R. Janson, J. J. Katz, In *The Porphyrins*, ed. by D. Dolphin, Academic Press (New York), 1978, Vol. IV, Chapter 1.
21. J. W. Buchler, In *The Porphyrins and Metalloporphyrins*, ed. by K. M. Smith, Elsevier Scientific Publishing (New York), 1975, Chapter V; M. Tsutsui, In *The Porphyrins and Metalloporphyrins*, ed. by K. M. Smith, Elsevier Scientific Publishing (New York), 1975, Chapter VII.
22. B. D. McLees and W. S. Caughey, *Biochemistry*, 1968, **7**, 642; R. J. Abraham and P. F. Swinton, *J. Chem. Soc. (B)*, 1969, 903; F. A. Walker, E. Hui, and J. M. Walker, *J. Am. Chem. Soc*., 1975, **97**, 2390.
23. In order to make the molecualr structures corresponding to respective spectral changes of OEP-DHBTh-PAR more confident, the quantitative analyses under various conditions are now investigation. Results of their electronic and electrochemical properties will be reported from the viewpoint of spectral and molecular motional reversibility in detail elsewhere.